National Research FLAGSHIPS Climate Adaptation

CSIRO

www.csiro.au

Analysis of Climate Change Impacts on the Deterioration of Concrete Infrastructure

Part 3: Case Studies of Concrete Deterioration and Adaptation

Australian Government

Department of Climate Change and Energy Efficiency

This report was prepared by Xiaoming Wang, Minh Nguyen, Michael Syme, Anne Leitch of CSIRO's Climate Adaptation Flagship, and Mark G. Stewart of the University of Newcastle, based on the research of 'An Analysis of the Implications of Climate Change Impacts for Concrete Deterioration', co-funded by Department of Climate Change and Energy Efficiency (DCCEE) and CSIRO Climate Adaptation National Research Flagship (CAF).

Part 1: Mechanisms, Practices, Modelling and Simulation – a Review
Part 2: Modelling and Simulation of Deterioration and Adaptation Options
Part 3: Case Studies of Concrete Deterioration and Adaptation.

Citation

Wang, X., Nguyen, M., Stewart, M.G., Syme, M., Leitch, A. (2010). Analysis of Climate Change Impacts on the Deterioration of Concrete Infrastructure – Part 3: Case Studies of Concrete Deterioration and Adaptation. Published by CSIRO, Canberra. ISBN 9780643103672

For Further Information

CSIRO Climate Adaptation Flagship
Dr Xiaoming Wang
Phone: 03 92526328
Fax: 03 92526246
Email: Xiaoming.Wang@csiro.au

Project Expert Panel

Important Disclaimer

Contents

ACKNOWLEDGMENTS 72

List of Figures

List of Tables

EXECUTIVE SUMMARY

Concrete structures are a key component of human settlement. Climate change is anticipated to have an impact on concrete structures through increasing rates of deterioration as well as through the impacts of extreme weather events. Understanding the implications of climate change on existing concrete structures is vital for effective asset planning and management undertaken by a range of governments and agencies. This is the third of three reports from a CSIRO project: *Analysis of Climate Change Impacts on the Deterioration of Concrete Infrastructure*, funded by both Department of Climate Change and Energy Efficiency (DCCEE) and CSIRO Climate Adaptation Flagship This project made theoretical and practical advances in analysing climate change impacts on the deterioration of concrete infrastructure.

In the first two reports in this series *Part 1: Mechanisms, Practices, Modelling and Simulations – A Review* and *Part 2: Modelling and Simulation of Deterioration and Adaptation Options* we outline current practices in concrete structure design and how climate change will affect the performance of concrete and therefore of built infrastructure that is designed on the implicit assumption of current or static climate conditions in existing standards. Such deterioration of concrete changes by direct and indirect impacts of climate change occurs predominantly through the corrosion of the concrete reinforcement.

In this third report we focus on the modelling and simulations for existing concrete infrastructure to explore adaptation options to reduce climate change impacts through case studies of concrete bridges and port structures. We build on the methodology outlined in the second report to present modelling and simulation for: deterioration of *existing* concrete structures based on field testing data integrated with probabilistic approaches; and various adaptation measures for chloride and carbonation induced corrosion. This modelling and simulation is tested through cases studies of 11 existing concrete bridges that were constructed in the period of pre-1959, 1959-1970, 1971-1994 within a temperate climate zone in New South Wales. A similar assessment is tested for concrete maritime structures in a tropical climate zone in a case study of the port of Townville. Adaptation options and their cost and benefits are discussed.

To simulate carbonation and corrosion through penetration of chloride in existing concrete we use a statistical method known as the Monte Carlo simulation. This approach considers environmental variables and their uncertainties, such as the concentration of carbon dioxide, yearly mean temperature and relative humidity as well as material properties. It is important to calibrate this approach through field testing using historical data of chloride concentration and carbonation penetration: this enables us to then project the probability of corrosion initiation and damage into future.

Modelling and simulation

Modelling and simulation were thoroughly discussed in the first two reports in this series, based on the assumption that the design of concrete structure meets the

Australian standard of *AS 3600 – concrete structures*. However, there needs to be more consideration on calibration of models for existing concrete structures to take into an account the uncertainties involved in individual structures on the aspects of their environmental exposure and service history. The field testing data are then used for the calibration.

For carbonation, the diffusion coefficient in the modelling is calibrated by the time of construction of concrete structures and the carbonation depth measured using a phenolphthalein pH indicator, in addition to historical environmental exposure. It is understood that testing methods may result in variability of the diffusion coefficient. Its uncertainties are then modelled by a normal distribution.

For chloride-induced corrosion, the corresponding diffusion coefficient and surface chloride concentration in Fick's law is calibrated by the chloride concentration profile along depth measured based on the British Standard BS 1881-Part 124 (1988) and considering the historical environmental exposure of individual structures. Chloride concentration variability is derived from the 95% confidence intervals to the best fit of the chloride concentration profile and is represented as a normal distribution.
Carbonation is also thought to accelerate chloride action but a lack of useful models for this interaction means that this is not explored in this report.

Modelling of adaptation measures for concrete, in many cases, is directly implemented by estimating the correction (multiplicative) factors that influence carbonation depth, diffusion coefficient, chloride concentration, critical chloride concentration or corrosion rate. Upon the review of previous researches, for example, carbonation depths reduction factor by acrylic-based surface coating is in the range of 25%-75%, chloride extraction may remove 20-90% of chloride concentration, and cathodic protection presumably removes all chloride ions from reinforcement making corrosion reduction rate none. If the original structure is simply replaced with new concrete, the subsequent deterioration process is considered to restart at the time of covering. Meanwhile, any coatings are considered to be adequately maintained during the life of the structure (i.e. coating will maintain the performance with time).

Climate Change Impacts on Existing Concrete Structures

Eleven existing bridges located within temperate climate zones in NSW are used as case studies of climate change impact on chloride-induced corrosion of the bridges. The bridges represent different construction periods at different regions including 1959, 1959-1970, 1971-1994, and post-1995. The profiles of chloride concentration were tested in 2008 at various locations of the bridges including more than one metre above the water level or spray zones (C1) and less than one metre above the water level or splash or tidal zones (C2). Port structures in a typical tropical climate zone are also field tested in the same way. Tested structures are concrete slab soffits and columns from a berth that is managed by Port of Townsville Limited.

This field test data is used to calibrate the diffusion coefficient and surface chloride concentration. This is used to project the probability of corrosion initiation and subsequent damage (including rebar loss) until 2100 with, and without, the effect of

climate change. It is also used to assess the performance of various adaptation measures.

Results of the field testing found, although all investigated structures are under exposure C2, the concrete cover does not necessarily meet the current standard (AS 3600-2009) that requires 65mm. In fact, the cover of the most of existing bridges in this case study is less than 65mm, with one reaching as low as 29mm. This emphasises how important it is to specifically assess the durability of existing bridges and especially when considering how climate change will affect concrete durability through carbonation- and chloride-induced corrosion.

Results also indicate that the effect of climate change on chloride-induced corrosion of concrete structures which design follows the AS3600 and AS5100.5, is within an increase of 3.5 percentage points in probability by 2100. In practice, the change of the probability can go higher due to non-binding on the standards or lack of quality assurance in construction, for example, use of lower concrete cover. The bridges in Sydney, constructed in 1925 with 29mm cover, shows that the climate change at A1FI emission scenario can leads up to an increase of 8 percentage points in corrosion initiation and damage probability value, or an equivalent increase of 13% in a percentage term. Even for a modern bridge in the northern region of NSW, constructed in 1984, the structure on the bridge at exposure C1 and C2 may experience up to 5-7 percentage point of increase in probability by 2100 in the presence of climate change impact at IPCC's A1FI emission scenario.

Due to an improper concrete cover of some of the early constructed bridges, climate change may lead to a considerable impact on carbonation-induced corrosion. For example, the bridge constructed in 1925 in Sydney has only 29mm concrete cover. The probability of corrosion initiation is 72, 67 and 63 percentage points by 2100 for A1FI, A1B and 550 ppm stabilisation emission scenarios, respectively, in comparison with 51 percentage points estimated in the absence of climate change. In other words, the probability increases 21, 16 and 12 percentage points in probability, or an equivalent increase of 41%, 31% and 14% in percentage terms due to climate change. Meanwhile, the probability of corrosion damage is 63, 60 and 55 percentage points in comparison with 44 percentage points estimated in the absence of climate change, also a significant increase due to climate change.

For a concrete column at exposure C2 in Port Townsville, climate change impact may lead to an increase of carbonation induced corrosion initiation probability from 1 percentage points to 45 percentage points for A1FI emission scenario, 28 percentage points for A1B emission scenario and 14 percentage points for 550 ppm stabilisation emission scenario by 2100. It also leads to an increase of corrosion damage probability from 0.2 percentage points to 16, 8.8 and 4.0 percentage points respectively for the three emission scenarios by 2100.

Adaptation options

Both chloride-induced and carbonation-induced corrosion show the potential experience of a scalable impact of climate change, which should be considered for maintenance

planning. Adaptation options should also be developed and optimised to mitigate the impact and enhance the adaptive capacity of concrete structures to changing climate.

A number of climate change adaptation options were simulated to determine their effectiveness. This included five options that are considered to reduce chloride-induced corrosion including electrochemical chloride extraction, polyurethane sealer, polymer-modified cementious coating, cover replacement and cathodic protection. It also included two options to reduce carbonation-induced corrosion including realkalisation and cover replacement.

Cost and adaptation effectiveness are also examined to quantify the adaptation options in order to identify the most preferable option for a specific concrete structure, such as a slab or column. The cost includes initial implementation cost and on-running operating cost, which are all converted to their present value in 2011 with a discount rate ranging from 1 to 10% selected for sensitivity assessment. The effectiveness, also known as a proxy of benefit due to the implementation of adaptation options, is defined as the amount of reduction in corrosion risk from 'business as usual (BAU)' after implementing adaptations. As a result, adaptation effectiveness is demonstrated by combining cost with adaptation effectiveness, which can support the decision-making for the most costs effective adaptation strategies. Meanwhile, the study indicates that the cost contributes to three factors, i.e. 1) reducing the impact of climate change, 2) increasing adaptive capacity to resist corrosion, and 3) offsetting the loss of adaptation effectiveness due to climate change. In general, the greater the offsetting in 3) the less effective is the option.

The case study of concrete bridges indicates that the replacement of concrete cover is often to be the most effective option, but it is also the most expensive one. Surface coating is the least costly, but is usually, not always, less effective. For the bridge constructed in 1925 in Sydney, cathodic protection is the preferred adaptation measure to mitigate the chloride-induced corrosion damage due to its greater effectiveness and moderate cost. Among the total cost, 22% is contributed to mitigate the increase corrosion damage risk due to climate change, 78% is contributed to increase adaptive capacity to resist corrosion, and nothing is contributed to offset the loss of adaptation effectiveness due to climate change. It should be pointed out the effectiveness of cathodic protection is in fact affected by sea level rise that may change the cost for offset the loss of effectiveness. At the same time, the use of polyurethane sealer is the least preferred due to its very low effectiveness though low cost. For this, 46% of the total cost is contributed to offset the loss, which is not really beneficial to the enhancement of adaptive capacity to counteract corrosion damage.

Depending on residual risk of corrosion damage of concrete structure after implementing adaptation options, the preferred adaptation option can vary. For a bridge constructed in 1967 in the northern region of NSW, polymer-modified cementious coating appears the most preferable due to its great effectiveness with 24% of the total cost is contributed to mitigate the increasing risk as a result of climate change, 57% is contributed to strengthen the adaptive capacity, and only 4% is contributed to offset the loss of adaptation effectiveness, in comparison with 14% for polyurethane sealer, 10%

for cathodic protection. Meanwhile, the cost is much lower than cover replacement, cathodic protection and chloride extraction.

A similar approach was applied for the cost/benefit assessment of adaptation options for carbonation-induced corrosion of port structures in relation to realkalisation and cover replacement are considered.

In summary this report shows that the climate change impact assessment of the aspect of design that follows the Australian standards may provide general rules for concrete structural design taking into account effects of changing climate. However, impacts on existing concrete infrastructure and the adaptation that should be applied to mitigate the impact are specific due to the uniqueness of individual structures especially regarding their different local environment exposure history as well as the uncertainties in construction and maintenance. Therefore, an effective adaptation option should be developed at the level of individual concrete structures. Finally, cost and benefit assessment should further be developed to consider the lifecycle of concrete infrastructure.

Bridge Construction (Source: CSIRO)

1. INTRODUCTION

The residual service life of existing concrete structures is largely determined by its deterioration over time. The deterioration rate of concrete structures depends not only on the construction processes employed and the composition of the materials used in the construction process, but also on the current as well as past environmental exposures. Meanwhile, climate change may alter this environment in the future, especially in the long term, causing more acceleration of deterioration processes and consequently affecting the safety and serviceability of existing concrete infrastructure. In particular, many existing concrete structures, for which the design has not taken into account the effect of changing climate, are likely to suffer from more decreased durability as a consequence of climate change and incur more damage and maintenance cost. Considering the amount of existing concrete infrastructure, the potential impacts of the climate change cannot be ignored.

As indicated in the previous part report, the deterioration of concrete can be affected directly or indirectly by climate change impacts, in association with the change in carbon dioxide (CO_2) concentration, temperature and relative humidity, as shown in Table 1-1. The climate-related deterioration of concrete structures is mostly caused by the infiltration of deleterious substances from the environment, for example carbon dioxide and chloride, which may cause reinforcement corrosion.

Understanding the implications of climate change on existing concrete structures is vital for effective decision-making in asset management to protect concrete buildings and infrastructure that underpin human settlements and the economy. In practice, the durability and serviceability of concrete structures are maintained via routine inspection, maintenance and replacement. Climate change impacts needs to be considered in both the application and effectiveness of maintenance and replacement regimes. Considering the extensive uncertainties and the limited knowledge of future climate, simulation is once again deemed as an effective approach that may provide insights into how likely

and how much the future climate would impact on existing concrete structures. More importantly, taking the precautionary principle, simulations may inform the necessary extent of change in maintenance required to maintain the safety, serviceability and durability given the likely climate change scenarios.

Table 1-1. Factors and potential consequences of climate change in association with concrete structures

Climate Change	Implications
Increase of carbon concentration	Elevated carbon concentration accelerates carbonation and increases carbonation depth in concrete: this increases the likelihood of concrete structures exposed to carbonation induced reinforcement corrosion initiation and structural damage
Change of temperature	Elevated temperature accelerates carbonation, chloride penetration and corrosion rate of reinforcement that exacerbates the corrosion damage
Change of humidity	Lowered relative humidity may reduce or even stop carbonation and chloride penetration in the area with yearly average RH currently just above 40-50%, while increased humidity may result in them occurring in the regions where they are now negligible.

This report will focus on the modelling and simulations for existing concrete infrastructure, and provide an effective way to explore adaptation options to reduce or mitigate the climate change impacts by case studies of concrete bridges and port structures.

In Chapter 2, we will establish methodology and present modelling and simulation for existing concrete deterioration based on field testing data integrated with probabilistic approaches. Models for the simulation of various adaptation measures for chloride and carbonation induced corrosion will also be introduced in the chapter (e.g. Stewart, 2010). Using modelling and simulation, cases studies will be carried out in Chapter 3 in relation to the climate change impact on existing concrete bridges constructed in the period of pre-1959, 19959-1970, 1971-1994 in Sydney, Southern, Northern as well as Hunter regions in NSW that are located within a temperate climate zone in Australia. The impact on chloride-induced corrosion will be represented by changes in mean corrosion initiation probability, corrosion damage probability and mean rebar loss. Climate change impact on carbonation-induced corrosion will also be addressed through the same concrete structures in NSW. In Chapter 4, a similar assessment will be carried out for concrete slabs and columns of port structures in the Port of Townsville that is located within a tropical climate zone in Australia. In Chapter 5, adaptation options to counteract or mitigate climate change impact on both chloride and carbonation induced corrosion will be discussed, and their cost and benefit will be presented in relation to the mitigation of climate change impact, increase of adaptive capacity and offset of adaptation effectiveness loss. Meanwhile, adaptation effectiveness diagrams will be developed for each case for decision-making on the selection of adaptation options in order to most cost-effectively maintain the durability and serviceability of bridges and port structures, which can be further extended to assess other concrete infrastructure.

Deteriorated concrete columns of bridge structures (source: RTA)

2. SIMULATION AND MODELLING OF EXISTING CONCRETE STRUCTURES

Simulation and modelling of carbonation and chloride induced corrosion for new structures have been discussed in great detail in the second part of the report. These simulations and models are based on the assumption that the design of concrete structures meets the Australian standard of AS3600 – Concrete Structures. Although these simulations and models are able to effectively project the overall performance of general deteriorating concrete structures from the aspect of a new design with consideration of changing climate, they could be inaccurate for the assessment of the performance of an individual existing concrete structure that can be different in practice as a result of uncertainties in construction and local environment as well.

The simulation of carbonation and chloride penetration induced corrosion of existing concrete is implemented by a conventional probabilistic approach on the basis of Monte-Carlo simulation, as demonstrated in the flow chart described in Figure 2-1. This approach considers dimensional, material properties and environmental variables and their uncertainties, including concentration of carbon dioxide, yearly mean temperature and relative humidity (Stewart, 2010). Different from the simulation described in the part 2 report, modelling of deterioration of existing individual concrete structures under changing climate should be calibrated by field testing data, as illustrated in the flow chart, so that corresponding climate adaptations can be properly developed. In this chapter, the procedure to modify the models developed in the previous report will be introduced to consider the characteristics of specific concrete structures. Meanwhile, the modelling of adaptations will also be developed for the assessment of their effectiveness to reduce the impact of climate change.

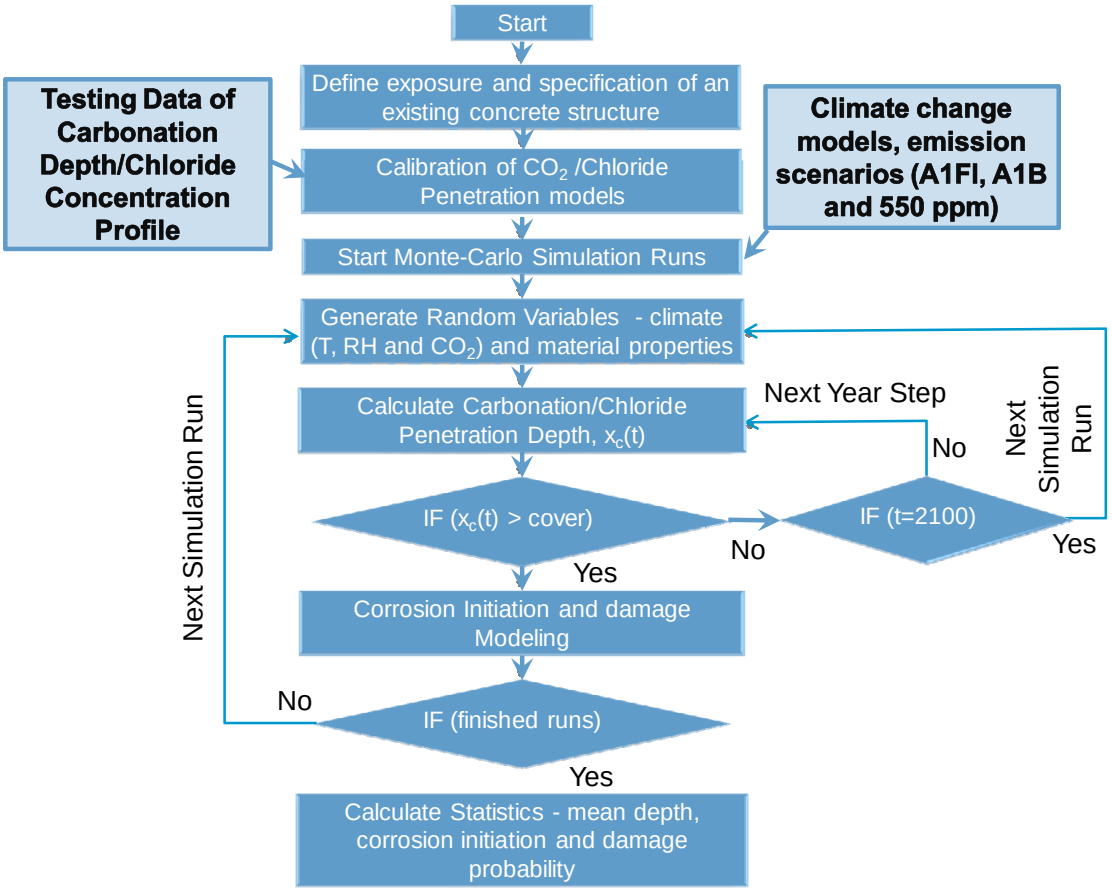

Figure 2-1 A flow chart of the simulation for the chloride and carbonation-induced corrosion of existing concrete structures

2.1 Carbonation-Induced Corrosion Modelling with Calibration by Field Testing Data

As discussed in the Part 2 – Modelling and Simulation of Deterioration and Adaptations, carbonation depth at calendar year t is described by

$$x_c(t) \approx \sqrt{\frac{2f_T(t)D_{CO_2}(t)}{a} k_{urban} \int_{2000}^{t} C_{CO_2}(t)dt} \left(\frac{t_o}{t-1999}\right)^{n_m} \qquad t \geq 2000 \qquad (2\text{-}1)$$

$$D_{CO_2}(t) = D_1(t-1999)^{-n_d} \qquad a = 0.75 C_e CaO \alpha_H \frac{M_{CO_2}}{M_{CaO}} \qquad \alpha_H \approx 1 - e^{-3.38 w/c} \qquad (2\text{-}2)$$

where t_o is the reference period (eg 1 year), t is time in years, $C_{CO_2}(t)$ is the time-dependent mass concentration of ambient CO_2 (10^{-3}kg/m^3) using the conversion factor 1 ppm (or ppmv) = 1.9×10^{-6} kg/m^3; $D_{CO_2}(t)$ is CO_2 diffusion coefficient in concrete; D_1 is

CO_2 diffusion coefficient after one year, are based on T=20 ^oC and RH=65%; n_d is the age factor for the CO_2 diffusion coefficient as shown in Table 2-1, and used for estimate other intermediate values by linear interpolation; C_e is cement content (kg/m^3); C_aO is CaO content in cement, 0.65 as used by the previous report if not specified; α_H is a degree of hydration; M_{CaO} is molar mass of CaO and equal to 56 g/mol and M_{CO_2} is molar mass of CO_2 equal to 44 g/mol. The age factor for microclimatic conditions (n_m) associated with the frequency of wetting and drying cycles is n_m=0 for sheltered outdoor and n_m=0.12 for unsheltered outdoor. k_{urban} is the CO_2 urbanisation factor; and $f_T(t)$ is the temperature factor.

Table 2-1 Ageing factor for CO_2 diffusion coefficient at given water/cement ratio (Yoon et al 2007).

w/c	n_d
0.45	0.218
0.50	0.235
0.55	0.240

For an existing concrete structure, Eqn. (2-1) can be calibrated by carbonation depth measurements. If carbonation depth x_{test} (cm) is known at time of test t_{test}, and the structure was constructed in the year t_{const}, then the equivalent first-year diffusion coefficient D_1 is

$$D_1 = \frac{a}{2f_T(t_{test})(t_{test}-t_{const})^{-n_d} k_{urban} \int_{t_{const}}^{t_{test}} C_{CO_2}(t)dt}\left[x_{test}\left(\frac{t_o}{t_{test}-t_{const}}\right)^{-n_m}\right]^2 \qquad t_{test} > 2000 \qquad (2\text{-}3)$$

$$f_T(t) \approx e^{\frac{E}{R}\left(\frac{1}{293}-\frac{1}{273+T_{av}(t)}\right)} \quad \text{where} \quad T_{av}(t) = \frac{\sum_{t_{const}}^{t} T(t)}{t-t_{const}} \qquad (2\text{-}4)$$

where T(t) is the temperature in ^oC, $f_T(t)$ is the temperature correction factor for diffusion coefficient, E=40 kJ/mol and R = 8.314×10^{-3} kJ/mol·K.

The CO_2 concentration in 1960 was $\mu_{CO2}(t)$ = 316 ppm, and is assumed to increase linearly to $\mu_{CO2}(t)$ = 369 ppm by 2000[1]. If time of test is before 1960 then CO_2 concentration is assumed constant at $\mu_{CO2}(t)$ = 316.0 ppm for all years to 1960. The variability of CO_2 concentration to year 2000 is zero, i.e., $\sigma_{CO2}(t) = 0$.

Based on the information from Bureau of Meteorology Australia, the median temperature increase due to global warming prior to 2000 will be less than after 2000.

[1] The carbon dioxide concentration in 1960 and 2000 is assumed on the basis of the information from record derived from spline smoothing of the DE08 and DE08-2 ice cores by Etheridge et al of CSIRO and CSIRO GASLAB Flask Sampling Network, which are available at Carbon Dioxide Information Analysis Centre (http://cdiac.ornl.gov).

For example, from 1950 to 2000 the median temperature increase was only 1.15 ^{o}C for Sydney. Simulation analyses have found that the best fit carbonation depth and chloride concentration are not significantly affected by pre-2000 temperature history (less than 1% in most cases). Hence, it is assumed that the mid global temperature change is $T_{mid-test}$=-1.0 ^{o}C in 1950 and temperature increases linearly until $T_{mid-test}$=0 ^{o}C in 2000. If time of test is before 1950 then $T_{mid-test}$ is assumed constant at $T_{mid-test}$=-1.0 ^{o}C for all years to 1950. The site-specific correction factor for temperature increase (k_{mid}) is omitted due to uncertainty about $T_{mid-test}$ prior to 2000. The mid temperature is $T(t)=T_{ref}+T_{mid-test}(t)$ where T_{ref} is the reference temperature at year 2000 and t<2000. If t>2000, then $T(t)=T_{ref}+[k_{mid}*T_{mid}(t)]$ where k_{mid} is the site-specific correction factor for temperature increase supplied by the user, and T_{mid} is the mid global temperature increase for the IPCC emission scenarios.

As known, carbonation is highest for RH=40-75%, or 50-70% (Russell et al 2001). Al-Khaiat and Fattuhi (2002) report that little or no carbonation occurs below a RH of 30%, whereas Russell et al (2001) state that below 50% RH there is insufficient moisture for carbonation reactions to take place. Most carbonation models assume RH>50%. To be conservative, assume that if RH(t) < 40% then carbonation front ceases to advance, or carbonation depth does not increase. Relative humidity prior to 2000 is likely to be well over 40% for most infrastructure locations in Australia, otherwise there would be no carbonation and no corrosion - and so no test results to analyse. Hence, relative humidity is not considered in the development of diffusion coefficient from test data.

Carbonation depths obtained using a phenolphthalein pH indicator are measured to an accuracy of ±0.5 mm (e.g., Al-Khayat et al. 2002, Jones et al. 2000). It follows that the diffusion coefficient D_1 is variable. If the test data describes a single carbonation depth x_{test} then we assume that D_1 is normally distributed, and there is a 95% probability that D_1 lies between those calculated for x_{test}±0.5 mm, then the standard deviation of D_1 (σ_{D1}) is $[D_1(x_{test}+0.5\text{ mm}) - D_1(x_{test}-0.5\text{ mm})]/3.92$. The mean of D_1 is based on diffusion coefficient calculated using x_{test} given by Eqn. (2-3).

If the test data describes a range of carbonation depths $x_{test(1)}$ and $x_{test(2)}$ then we assume that mean(D_1) is based on $x_{test}=(x_{test(1)}+x_{test(2)})/2$ and if D_1 is normally distributed, and there is a 95% probability that D_1 lies between those calculated for $x_{test(1)}$ and $x_{test(2)}$, then $\sigma_{D1}= [D_1(x_{test(2)}) - D_1(x_{test(1)})]/3.92$.

For times less than t_{test} it is assumed that σ_{D1}=0 and Coefficient of Variation (COV) of k_{urban} is zero. For all times COV for n_d is zero as the best fit for diffusion coefficient will minimise any carbonation depth model errors and so minimise parameter variability.

It is recognised that carbonation test methods may result in variability in test measurements (e.g., Jones et al. 2000). However, test measurements based on averaging several sample results should minimise these uncertainties. The present analysis assumes that the carbonation depth obtained using a phenolphthalein pH indicator is an accurate indicator of carbonation.

The carbonation depth for times greater than t_{test} is predicted as:

$$x_c(t) \approx \sqrt{\frac{2f_T(t)D_{CO_2}(t)}{a} k_{urban} \int_{t_{const}}^{t} C_{CO_2}(t)dt} \left(\frac{1}{t - t_{const}}\right)^{n_m} \qquad t \geq t_{test} \geq 2000 \tag{2-5}$$

$$D_{CO_2}(t) = D_1\left(t - t_{const}\right)^{-n_d} \tag{2-6}$$

where a, α_H and $f_T(t)$ are given by Eqns. (2-2) and (2-4).

It is observed that corrosion may occur when the distance between the carbonation front and the reinforcement bar surface is less than 1-5 mm (e.g., Yoon et al 2007). However, probabilistic analyses for assessing durability design specifications tend to ignore this effect (Duracrete 2000b, fib 2006). Hence, time to corrosion initiation (T_i) occurs when carbonation front equals concrete cover, and the probability of corrosion initiation is given by:

$$p_i(t') = \Pr\left[h - x_c(t') < 0\right] \tag{2-7}$$

where *h* is the cover thickness.

2.2 Chloride-Induced Corrosion Modelling with Calibration by Field Testing Data

There is evidence to suggest that chloride action is accelerated by carbonation (and SO_2, NO_x) because carbonation disturbs the equilibrium between free and bound chlorides in the concrete, thereby increasing the free chloride concentration in the pore solution. However, it appears that this evidence has not been translated into any useful quantitative models. Thus the interaction effect between carbonation and chlorides is, for the time being, omitted from the present study. Use total (acid soluble) chloride content.

The British Standard BS 1881-Part 124 (1988) "Testing concrete - Part 124: Methods for Analysis of Hardened Concrete" is used for assessing total chloride content. Within the U.K. this is seen as the 'reference' method (Bamforth et al. 1997). While the test method is accurate, there is little information about variability of test results from 'identical' specimens.

Chloride content C(x,t) is obtained for specimens typically of 10 to 20 mm depth, and the mid-height value of each slice (x) is used when determining chloride profiles at time t (e.g., McGee 1999, Tamimi et al 2008).

Chloride penetration based on Fick's law is

$$C(x,t) = C_0 - \left(C_0 - C_i\right)\operatorname{erf}\left(\frac{x}{2\sqrt{D_c(t - 1999)}}\right) \qquad t \geq 2000 \tag{2-8}$$

where C_o is the surface chloride concentration, C_i is the initial chloride concentration that already exists in the concrete mix, D_c is the chloride diffusion coefficient, and x is depth of concrete specimen.

Most durability studies, including Duracrete (2000a) assume that initial chloride concentration C_i is zero. However, Polder and de Rooij (2005) and Kershel (2009) show that chloride measurements in the tail of the chloride profile may be considerably higher and for a better fitting result C_i is non-zero. This is due to small, though often acceptable, chloride concentrations in mixing water and aggregates. For example, Kershel (2009) found that chloride content taken at 120 mm from the surface of a bridge in Ireland had chloride levels of 0.011% (by mass of concrete), and Polder and de Rooij (2005) reported values of C_i= 0.01%. The effect of C_i on curve fitting will be illustrated later in this Section.

The diffusion coefficient is time-dependent due to the continuing densification of the concrete microstructure as a result of the continuing hydration of the cement. Hence, the following power function is used (eg. Duracrete 2000a):

$$D_c(t) = D_{c-o}\left(\frac{t_o}{t - t_{const}}\right)^n = D_{c-o}\left(\frac{t_{test} - t_{const}}{t - t_{const}}\right)^n \quad t \geq t_{test} \geq 2000 \tag{2-9}$$

where D_{c-o} is the reference diffusion coefficient at a reference time t_o (age of structure at time of test) and n is the age reduction factor which depends mainly on mix proportions of the concrete. The age reduction factor (n) is approximately 0.2, 0.4 and 0.6 for OPC, PFA and GGUBS concrete, respectively (Kershel 2009).

Non-linear least squares methods are used to determine the 'best fit' Fick's law parameters for diffusion coefficient D_{c-o} and surface chloride concentration C_o from Eqns. (2-8) and (2-9). Considering $t=t_{test}$ and time t_o is equal to the age of structures at time of test (t_{test}-t_{const}), Eqn. (2-8) can be rewritten as:

$$C(x, t_{test}) = C_o - (C_o - C_i)\,\mathrm{erf}\left(\frac{x}{2\sqrt{f_T(t_{test})D_{c-o}(t_{test} - t_{const})}}\right) \quad t_{test} \geq 2000 \tag{2-10}$$

where $f_T(t)$ is given by Eqn. (2-4). Note that environment, curing and test factors described in Duracrete (2000a) are assumed as unity for the purposes of best-fit calculations.

As a result, chloride concentration can then be predicted at any time t as:

$$C(x,t) = C_o - (C_o - C_i)\,\mathrm{erf}\left(\frac{x}{2\sqrt{f_T(t)D_{c-o}\left(\frac{t_{test} - t_{const}}{t - t_{const}}\right)^n (t - t_{const})}}\right) \quad t \geq t_{test} \geq 2000 \tag{2-11}$$

The 95% confidence intervals to the best fit profile and regression coefficient (R^2) are obtained from standard statistical methods (Ang and Tang 2007). The value of initial chloride concentration (C_i) can be varied by the user to improve the fit by maximising the regression coefficient. As part of the least squares regression analysis, the user is required to input initial (guess) parameters for $D_{c\text{-}o}$ and C_o - suggested initial values are $D_{c\text{-}o}$=0.5 and C_o=highest sample concentration. If the best fit parameters fail to converge then other initial values should be used until convergence occurs.

The variability of chloride concentration will be derived from the 95% confidence intervals to the best fit profile. If it is assumed that chloride concentration variability is represented as a normal distribution, then the 95% confidence intervals represent a deviation from the mean of $1.96\sigma_C$ where σ_C is the standard deviation of chloride concentration. In addition, in all cases the age factor (n) is kept at a constant value (n=0.2 for OPC) for simplicity in simulation, though it may only be taken as approximation for other types of concrete.

It is expected that chloride concentration will reduce as depth increases. However, chloride concentrations in the top few mm of the concrete cover may be lower because the concrete skin has a different composition compared to the internal concrete. This "skin effect" can be due to contact with formwork, segregation of aggregates, dielectric reactions between the concrete surface and chloride environment, or chlorides at the surface may be washed out in preparation of sampling (e.g., Andrade et al 1997, Song et al. 2008). If the chloride concentration is lower for the lowest sample depth then this indicates a "skin effect" and this measurement should be omitted from the best fit statistical analysis.

In addition, the statistics of critical chloride concentration (C_{cr}) are mean = 3.35 kg/m^3, COV=0.375, truncated at 0.35 kg/m^3 - normal distribution (Val and Stewart 2003). These statistics are not affected by concrete quality (Duracrete 2000a). In this regard, the time to corrosion initiation (T_i) occurs when chloride concentration exceeds critical chloride concentration (C_{cr}), and the probability of chloride-induced corrosion is:

$$p_i(t') = \Pr[C(h,t)\text{-}Cr < 0] \qquad (2\text{-}12)$$

2.3 Cover Measurement

Data analysis of carbonation and chloride levels often also includes cover measurements. A covermeter is typically used for these measurements. The British Standard BS1881-Part 204 (1988) "Testing Concrete: Recommendations on the Use of Electromagnetic Covermeters" states that the indicated cover to steel reinforcement by a calibrated covermeter should be accurate to with ±5% or ±2 mm, whichever is the greater, over the working range given by the manufacturer. A study by Barnes and Zheng (2008) found that all the measured covers were well within ranges specified by BS1881. This study will assume the same accuracy levels for covermeters as BS1881-Part 204 (1988). Hence, assuming a normal distribution and that 95% of covers lie

within covermeter accuracy, then the standard deviation is the greater of 2/1.96 mm or 0.05×cover/1.96.

2.4 Modelling of Adaptations for Existing Structures

An adaptation may influence carbonation depth, chloride diffusion coefficient, chloride concentration, corrosion rate, or critical chloride concentration if the existing concrete cover is not replaced. If the existing concrete cover is replaced with new concrete then in this case the deterioration process of the existing structure ceases and the deterioration process restarts at the time of cover replacement at time t_{adapt}.

It assumes that any coatings are adequately maintained during the life of the structure (ie. coating will maintain the performance with time). In most cases, an adaptation can be directly simulated by the estimation of correction (multiplicative) factors (R) that influence carbonation depth, diffusion coefficient, chloride concentration, critical chloride concentration or corrosion rate.

2.4.1 Carbonation Depth Factor (R_{carb})

Reduction in carbonation depth only applies when t exceeds t_{adapt}, hence the carbonation depth multiplicative factor (R_{carb}) applies only to the incremental increase in carbonation depth each year, namely, carbonation depth is

$$\begin{aligned} x_c(t) &= x_{c(1)}(t) && t < t_{adapt} \\ x_c(t) &= x_c(t-1) + R_{carb}\left[x_{c(1)}(t) - x_{c(1)}(t-1)\right] && t \geq t_{adapt} \end{aligned} \tag{2-13}$$

where $x_{c(1)}$ is the carbonation depth assuming no adaptation measures (R_{carb}=1.0). For example, a carbonation depth multiplicative factor (R_{carb}) of 0.5 to carbonation depth means that calculated corrosion depths are multiplied by 0.5.

Researches indicated that an acrylic-based surface coating causes 10-65% reduction in carbonation based on nine week tests (Ho and Harrison 1990). If a minimum of two coats were applied then the minimum reduction in carbonation depth is 25% (Ho and Harrison 1990). It is reported that there was 60-83% reduction in carbonation depth on the basis of a 2.5 year test (Swamy et al. 1998). Moreno et al (2007) found an 85% reduction in carbonation depth, 64 days after acrylic and 'good quality' vinyl-acrylic coatings, but indicated that most vinyl-acrylic coatings had smaller reductions in carbonation depth. In addition, it is found that silicone coating has no reduction effect on carbonation depth (Ho and Harrison 1990).

In general, acrylic-based surface coating appears most effective in dry environments, and should not be used in wet environments (Exposures C, C1 and C2). Meanwhile, treatment should be uniformly applied with the minimum number of defects. In the

simulation of coatings for existing concrete structures, it is assume that the reduction in carbonation depths is in the range of 25%-75%, or R_{carb}=0.25-0.75.

2.4.2 Chloride Diffusion Factor (R_D)

Reduction in chloride diffusion coefficient only applies when t exceeds t_{adapt}, hence the chloride diffusion multiplicative factor (R_D) applies only to the incremental increase in chloride concentration each year, namely, chloride concentration at time t is

$$C(x,t) = C_o - (C_o - C_i)\,\mathrm{erf}\left(\frac{x}{2\sqrt{f_T(t) D_{c-o}\left(\frac{t_{test} - t_{const}}{t - t_{const}}\right)^n (t - t_{const})}}\right) \qquad t < t_{adapt}$$

$$C(x,t) \approx C_o - (C_o - C_i)\,erf\left(\frac{x}{2\sqrt{f_T(t)\left(\frac{t_{test} - t_{const}}{t - t_{const}}\right)^n \left[D_{c-o}(t_{adapt} - t_{const} - 1) + R_D D_{c-o}(t - t_{adapt} + 1)\right]}}\right) \qquad t \geq t_{adapt} \tag{2-14}$$

where D_{c-0} is the chloride diffusion coefficient assuming R_D=1.0. Eqn. (2-14) is an approximation, and aims to reflect the time integration of diffusion coefficient within the error function.

Surface treatments aim to reduce the chloride diffusion coefficient: and they should be applied before corrosion initiation. The effective diffusion coefficient considering surface coating is described by (Buenfeld and Zhang 1998):

$$D_e = \frac{T_c + T_{ST}}{\left(\frac{T_c}{D_c} + \frac{T_{ST}}{D_{ST}}\right)} \tag{2-15}$$

T_c = concrete cover
T_{ST} = thickness of surface treatment
D_c = chloride diffusion coefficient without surface treatment
D_{ST} = chloride diffusion coefficient of surface treatment

Table 2-2 Parameters of surface coatings

Surface Treatment	T_{ST} (mm)	D_{ST} (10^{-12} m^2/s)
Polyurethane sealer	0.02 mm	1.4×10^{-3}
Silane	2 mm	2.5×10^{-1}
P-m (Polymer modified) cementitious coating	1.5 mm	6.3×10^{-3}

Note: $D_c=3\times10^{-12}$ for tests used to determine D_{ST}.

An acrylic coating reduces diffusion coefficient by 50% (R_D=0.5), and a two component epoxy resin reduced diffusion coefficient by 100% (R_D=0.0) (Aguair et al. 2008).

2.4.3 Chloride Concentration Factor ($R_{chloride}$)

Reduction in chloride concentration only applies when t exceeds t_{adapt}, hence the chloride concentration multiplicative factor ($R_{chloride}$) applies only to the incremental increase in chloride concentration each year, namely, chloride concentration is

$$C(x,t) = C(x,t)_{(1)} \qquad t < t_{adapt}$$

$$C(x,t) = C(x,t-1) + R_{chloride}\left[C(x,t)_{(1)} - C(x,t-1)_{(1)}\right] \qquad t \geq t_{adapt} \tag{2-16}$$

where $C(x,t)_{(1)}$ is the chloride concentration assuming no adaptation measures ($R_{chloride}$=1.0).

Electrochemical Chloride Extraction removes some chlorides from concrete cover. Sharp et al (2002) in a review of U.S. chloride extraction studies (bridge decks and piers) found that chloride extraction removed 20-90% of chlorides. Schneck et al. (2007) found a 70% reduction in chloride content, and Velivavaskis et al. (1998) reported 40-80% reduction from case studies taken from U.S. bridges. An experimental study found that 33-76% of chlorides were removed (Sharp et al 2002). Carbonation will reduce chloride extraction rate (Ihekwaba et al 1996) and so a lower limit of 30% extraction may be appropriate ($R_{chloride}$=0.7).

2.4.4 Critical Chloride Concentration Factor (R_{cr})

The critical chloride concentration multiplicative factor (R_{cr}) is applied to the critical chloride concentration (C_{cr}) as

$$C_{cr} = C_{cr} \qquad t < t_{adapt}$$

$$C_{cr} = R_{cr}C_{cr} \qquad t \geq t_{adapt} \tag{2-17}$$

Corrosion Rate Factor (R_{icorr})

The corrosion rate multiplication factor (R_{icorr}) is applied to the corrosion rate at T=20 ^{o}C as

$$i_{corr-20} = i_{corr-20} \qquad t < t_{adapt}$$
$$i_{corr-20} = R_{icorr} i_{corr-20} \qquad t \geq t_{adapt} \tag{2-18}$$

The corrosion rate factor is applied to simulate realkanisation. Realkanization is an electrochemical process to raise pH near reinforcement. After realkanization then concrete will not easily recarbonate and so the effect tends to be permanent (Velivavaskis et al. 1998). Yeih and Chang (2005) report that the corrosion rate becomes negligible (<0.1 $\mu A/cm^2$) after realkanization. Hence, in the simulation, the corrosion rate factor R_{icorr}=0.0.

Surface coatings may also reduce corrosion rate because of reduced moisture ingress into concrete (Bentur et al. 1997; Ibrahim et al. 1999). However, it will be assumed no effect on corrosion rate in the simulation, i.e. R_{icorr}=1.0.

Cathodic Protection is assumed to be 100% effective in removing chloride ions from reinforcement, and therefore result in R_D=0.0 and R_{icorr}=0.0.

Chloride extraction will lower corrosion rate by 60-90% (Velivavaskis et al. 1998), and Broomfield (1997) states 'very low corrosion rates' even if chloride levels are above the critical chloride content. It is therefore assumed that R_{icorr}=0.5 for the simulation.

2.4.5 Replace Existing Cover with New Concrete

The existing concrete cover is removed and replaced with new concrete. In this case, the deterioration process of the existing structure ceases and the deterioration process restarts at the time of cover replacement at time t_{adapt}. It is assumed that (i) the new concrete cover re-passivates the steel reinforcement (corrosion rate is zero), (ii) corrosion loss of reinforcement is not rectified at time of cover replacement, and (iii) if corrosion initiates the corrosion rate is the same as for the original concrete cover (i.e. not affected by the new concrete cover).

The carbonation depth at time t is:

$$x_c(t) \approx \sqrt{\frac{2 f_{TA}(t) D_{CO_2}(t)}{a} k_{urban} \int_{t_{adapt}}^{t} C_{CO_2}(t) dt \left(\frac{1}{t - t_{adapt}} \right)^{n_m}} \qquad t \geq t_{adapt} \geq 2000 \tag{2-19}$$

$$D_{CO_2}(t) = D_1 \left(t - t_{adapt} \right)^{-n_d} \qquad a = 0.75 C_e CaO \alpha_H \frac{M_{CO_2}}{M_{CaO}} \qquad \alpha_H \approx 1 - e^{-3.38 w/c} \tag{2-20}$$

$$f_{TA}(t) \approx e^{\frac{E}{R}\left(\frac{1}{293} - \frac{1}{273 + T_{av-A}(t)} \right)} \qquad \text{where } T_{av-A}(t) = \frac{\sum_{t_{adapt}}^{t} T(t)}{t - t_{adapt}} \tag{2-21}$$

where parameters w/c, C_e, D_1 and n_d are suggested in Table 2. The standard deviation for D_1 is approximately 0.15, and COV for n_d is approximately 0.12 for all w/c ratios. These statistics represent model error (or accuracy). However, the user may select statistical parameters according to their own experience.

Table 2-3 Input Parameters for New Concrete Cover, for Carbonation

F'$_c$ (MPa)	w/c[d] ratio	C_e[a] (kg/m^3)	mean D_1 ($\times 10^{-4}$ cm^{2}s^{-1})	mean n_d
20	0.56	320	2.22	0.240
25	0.56	320	2.22	0.240
32	0.50	320	1.24	0.235
40	0.46	370	0.65	0.218
50	0.40	420	0.47[b]	0.19[c]

Notes - a: based on minimum cement content specified in AS 5100.5, b: conservative value, c: conservative value, d: based on maximum w/c ratio specified in AS 5100.5.

The chloride concentration at time t is (Duracrete 2000a):

$$C(x,t) = C_o\left[1 - \mathrm{erf}\left(\frac{x}{2\sqrt{k_e \bullet f_{TA}(t) D_c \left(\frac{t_o}{t - t_{adapt}}\right)^n \bullet \left(t - t_{adapt}\right)}}\right)\right] \qquad t \geq t_{adapt} \geq 2000 \qquad (2\text{-}22)$$

where t_o is 28 days (0.0767 years), f_{TA} is given by Eqn. (18), and D_c, n, k_e and C_o are given in Tables 3 and 4. Since statistical parameters given in Table 3 are sourced from Duracrete (2000a) which is based on Fick's Law with C_i=0.0%, then the same formulation of Fick's Law is used herein. However, the user may select statistical parameters according to their own experience.

Table 2-6 and Table 2-7 summarise the factors selected for the simulation of various adaptation measures described previously, which are in fact the traditional maintenance techniques, for carbonation- and chloride-induced corrosion.

Table 2-4 Input Parameters for New Concrete Cover, for Chlorides

Exposure Descriptions	Exposure Classification	F'c (MPa)	w/c[b] ratio	mean(D_c) $\times 10^{-12}$ COV=0.285	mean(n) σ=0.07	mean(k_e) SD
Members in exterior environments						
Near-coastal (1-50 km), any climate	B1	32	0.50	15	0.65	0.676 σ=0.114
Coastal (up to 1 km, excluding tidal and splash zones), any climate	B2	40	0.46	10	0.65	0.676 σ=0.114
Surfaces of members in water						
splash and tidal zones	C	50	0.40	7	0.37	0.924 σ=0.155
in spray zone (>1 m above wave crest level)	C1[e]	50	0.40	7	0.37	0.265 σ=0.045
splash and tidal zones	C2[e]	50	0.40	7	0.37	0.924 σ=0.155

Notes - b: based on maximum w/c ratio specified in AS 5100.5, e: New Concrete Structures Code - AS3600-2009 (based on draft D05252 (2005)).

Table 2-5 Surface Chloride Concentration C_o (Val and Stewart 2003).

Environment Exposure Descriptions	Mean	COV	Distribution
Splash/Tidal Zone	7.35 kg/m^3	0.7	Lognormal
Atmospheric Zone on the Coast	2.95 kg/m^3	0.7	Lognormal
Atmospheric Zone >1 km from the Coast	1.15 kg/m^3	0.5	Lognormal

Table 2-6 Selection of various factors of adaptation measures for carbonation-induced corrosion

Adaptation measures	carbonation depth factor [R_{carb}]	carbonation diffusion factor [R_D]	corrosion rate factor [R_{icorr}]
acrylic-based surface coating	0.25-0.75	1	1
realkanization	1	1	0
replace existing cover	1	1	1

Table 2-7 Selection of various factors of adaptation measures for chloride-induced corrosion

Adaptation measures	chloride concentration factor [$R_{chloride}$]	chloride diffusion factor [R_D]	critical chloride concentration factor [R_{cr}]	corrosion rate factor [R_{icorr}]
acrylic coating	1	0.5	1	1
epoxy resin coating	1	0	1	1
cathodic protection and concrete replacement	1	0	1	0
electrochemical chloride extraction	0.7	1	1	0.5
replace existing cover	1	1	1	1

Cracked concrete bridge structures (source: RTA)

3. CLIMATE CHANGE IMPACT ON CORROSION OF EXISTING CONCRETE BRIDGE STRUCTURES IN TEMPERATE CLIMATE ZONES

3.1 Chloride-Induced Corrosion of Concrete Bridges

3.1.1 Bridges for Chloride-Induced Corrosion Assessment

Eleven existing bridges located within temperate climate zones in NSW are used as case studies of climate change impact on chloride-induced corrosion of the bridges. The bridges were chosen as representative of different construction periods at different regions, as shown in Table 3-1. The construction periods of bridges are divided into groups of prior to 1959, 1959-1970, 1971-1994, and post-1995. The data of post-1995 bridge structures is not available.

The profiles of chloride concentration were tested in 2008 at various locations of the bridges, and the test results are reported by (RTA, 2008). In this study, analysis will be carried out for the location where the core sample shows the highest chloride concentration among all the test samples of the each bridge at the same exposure. For example, as shown in Table 3-1, the selected samples for the bridges are given by in the report (RTA, 2008), and C1 is the exposure class of the sample. Exposure C1 is for locations more than 1m above the water level or spray zones, and exposure C2 is for locations less than 1m above the water level or splash and tidal zones.

The field test data is then applied to calibrate the diffusion coefficient and surface chloride concentration, as indicated in the previous chapter, which are then used to project the corrosion until 2100 with the effect of climate change or not, as well as the influence of various adaptation measures.

Table 3-1 List of bridges assessed for corrosion due to chloride penetration

Construction Period	Region			
	Southern	Sydney	Hunter	Northern
Pre-1959	**Bridge BA1** Built year: 1956 Exposure: C1 Cover: 55mm	**Bridge BB1** Built year: 1925 Exposure: C1 Cover: 29mm	**Bridge BC1** Built year: 1940 Exposure: C1 Sample: M1 (C2) Cover: 50mm	**Bridge BD1** Built year: 1943 Expsoure: C2 Cover: 70mm
1959 – 1970	**Bridge BA2** Built year: 1959 Exposure: C2 Cover: 50mm	**Bridge BB2** Built year: 1959 Exposure: C1 Cover: 48mm	**Bridge BC2** Built year: 1968 Exposure: C2 Cover: 53mm	**Bridge BD2** Built year: 1967 Exposure: C2 Cover: 62mm
1971 – 1994	**Bridge BA3** Built year: 1980 Exposure: C2 Cover: 58mm	*Test data not available*	**Bridge BC3** Built year: 1989 Exposure: C2 Cover: 67mm	**Bridge BD3** Built year: 1984 Exposure: C1/C2 Cover: 62mm
Post-1995	*Test data not available*	*Test data not available*	*Test data not available*	*Test data not available*

3.1.2 Pre-1959 Bridge Structures

Bridge BA1 (1956, Southern Region)

Bridge BA1, as shown Figure 3-1, is constructed in the pre-1959 period and by 2008 has been in service for 52 years with fairly extensive corrosion and damage at the inspected location under exposure C1.

Figure 3-1 Bridge BA1 constructed in 1956 in the southern region of NSW (Source: RTA)

The probability of corrosion initiation was 48 percentage points by 2000, and the corresponding probability of corrosion damage was 36 percentage points and the mean rebar loss was around 0.55 mm. They are now estimated to be 62%, 52% and 0.97mm, respectively. If left untreated, the probability of corrosion initiation and damage increases to above 97 percentage points by 2100 in all three climate change scenarios. Thus it is almost certain that the bridge will experience damage, as shown in Figure 3-2. The effect of climate change on the probability is within 1 percentage points, and the effect on rebar loss within 1.2mm by 2100 (or an equivalent 13% increase of the mean rebar loss in the absence of climate change). In fact, the very severe chloride-induced corrosion on this bridge structure has subdued the effect of changing climate. It would be more worthwhile to assess the impact of adaptation measures that are applied to ameliorate the deterioration caused by the corrosion.

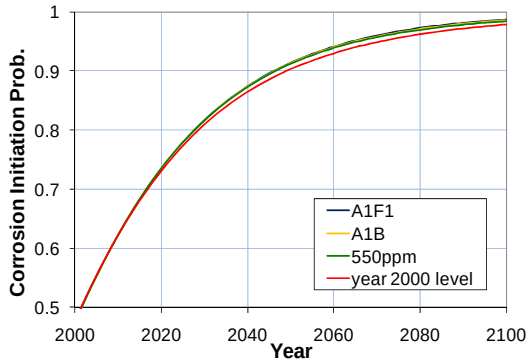

(a) Corrosion initiation probability

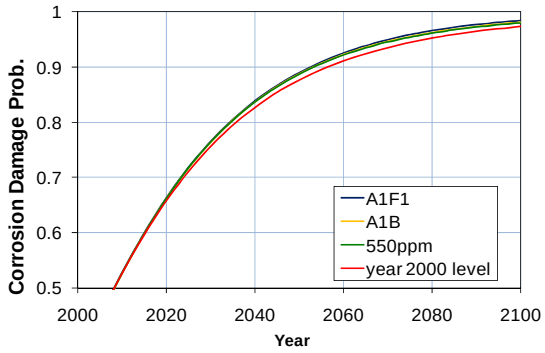

(b) Corrosion damage probability

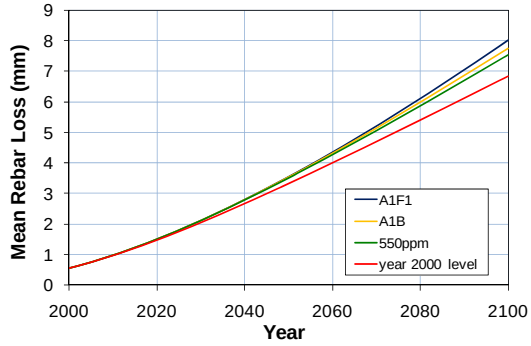

(c) Mean rebar loss (mm)

Figure 3-2 The probability of chloride-induced corrosion initiation and damage and mean rebar loss of Bridge BA1 in a temperate climate zone, with the effect of climate change in comparison with the baseline in the absence of climate change. 'year 2000 level' is the relevant value in the absence of climate change. (The probability is represented by decimal numbers)

Bridge BB1 (1925, Sydney) and BB2 (1959, Sydney)

Concrete structures on bridges built in 1925 and 1959 were assessed as shown in Figure 3-3. One built in 1959 shows very low corrosion risk at a location with exposure C1 as the probabilities of corrosion and the mean rebar loss were negligibly small at the time of testing in 2008. However, one built in 1925 shows the probability of chloride-induced corrosion initiation and damage at 14 and 12 percentage points by 2008, respectively. The corresponding mean rebar loss is 0.25mm.

The probability of corrosion initiation is projected to be 70, 68 and 67 percentage points for A1FI, A1B and 550 ppm stabilisation emission scenarios by 2100, respectively, in comparison with 62 percentage points in the absence of climate change, as shown in Figure 3-4. The probability of corrosion damage is projected to be 68, 66 and 65 percentage points for the three emission scenario respectively in comparison with 60% percentage points in the absence of climate change. The mean rebar loss is 3.7mm, 3.5mm, and 3.4mm for the three emission scenarios respectively in comparison with 2.9mm in the absence of climate change. Therefore, the effect of climate change on the probability of chloride-induced corrosion initiation and damage is within an 8 percentage points increase in probability, (or an equivalent 13 increase in a percentage term) and the effect on the mean rebar loss is within 0.8mm increase by 2100, for the three emission scenarios.

Figure 3-3 Bridge BB1 constructed in 1925 and 1959, in Sydney (Source: RTA)

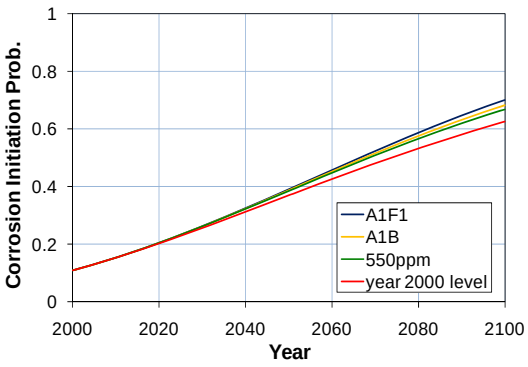

(a) Corrosion initiation probability

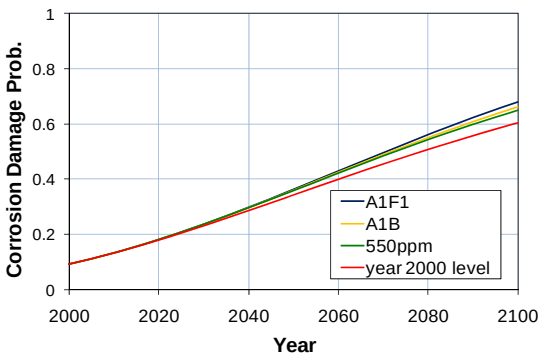

(b) Corrosion damage probability

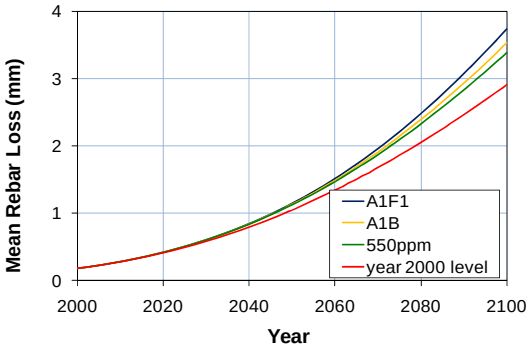

(c) Mean rebar loss (mm)

Figure 3-4 The probability of chloride-induced corrosion initiation and damage and mean rebar loss of Bridge BB1(1925) in a temperate climate zone, with the effect of climate change in comparison with the baseline in the absence of climate change. 'year 2000 level' is the relevant value in the absence of climate change. (The probability is represented by decimal numbers)

Bridges BC1 (1940, Hunter Region)

Bridge BC1 has been in service for 68 years to 2008, as shown in Figure 3-5, the tested structures are exposed to C1 and C2 classes, respectively. The structure at a location of the bridge under exposure C1 shows very low corrosion in terms of the negligible probability of corrosion initiation and damage as well as mean rebar loss.

Figure 3-5 Bridge BC1 constructed in 1940, in Hunter region of NSW (Source: RTA)

The structure at a location with exposure C2, however, shows considerable likelihood of chloride-induced corrosion. The probabilities of corrosion initiation and damage were very high at 54 and 49 percentage points , respectively, and the mean rebar loss is 2.0mm by 2008. As shown in Figure 3-6, the probability of corrosion initiation and damage is above 99 percentage points , or almost certain by 2100. The corresponding mean rebar loss is 18mm in comparison with 16mm in the absence of climate change. The significance of the corrosion rate subdues the effect of climate change on corrosion initiation and damage that become almost certain anyway by 2100. It would be more important to consider the impact of climate change on maintenance measures that are applied to reduce the corrosion-induced structural deterioration. However, climate change is projected to cause up to 2.2mm increase in mean rebar loss by 2100, or 14 percentage points increase in comparison with the rebar loss in the absence of climate change.

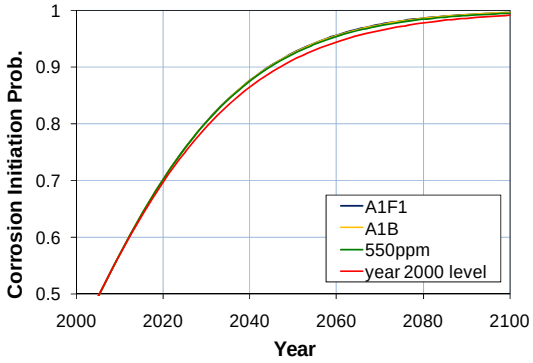

(a) Corrosion initiation probability

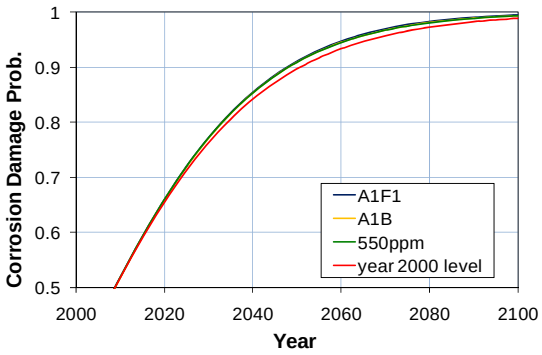

(b) Corrosion damage probability

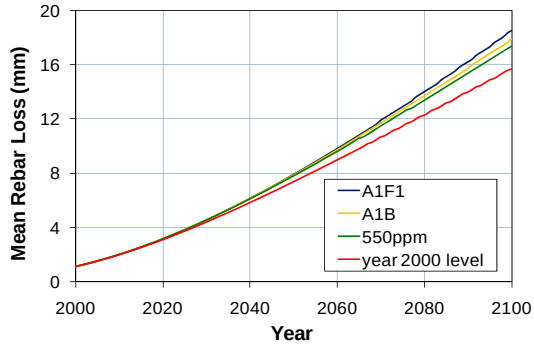

(c) Mean rebar loss (mm)

Figure 3-6 The probability of chloride-induced corrosion initiation and damage and mean rebar loss of Bridge BC1 in a temperate climate zone, with the effect of climate change in comparison with the baseline in the absence of climate change. 'Year 2000 level' is the relevant value in the absence of climate change. (The probability is represented by decimal numbers)

Bridge BD1 (1943, Northern Region)

Bridge BD1 has been in service for 65 years to 2008, the structure at a location under exposure C2 was tested and applied to calibrate the corrosion models. It shows moderate corrosion in 2008 with the probabilities of corrosion initiation at 23 percentage points , the probability of corrosion damage at 20 percentage points , and the mean rebar loss at 1.1mm by 2008. It may be partially contributed by the high cover thickness of 70mm.

As shown in Figure 3-7, the probability of corrosion initiation is projected to increase to 79, 77 and 76 percentage points by 2100 for A1FI, A1B and 550 ppm stabilisation emission scenario in comparison with 73% in the absence of climate change. The probability corrosion damage is 77, 76, and 75 percentage points by 2100 for the three emission scenarios in comparison with 71 percentage points in the absence of climate change. The mean rebar loss is 11.2mm, 10.7mm, and 10.3mm for the three emission scenarios, respectively, in comparison with 9.1mm in the absence of climate change. In this regard, climate change may lead to an increase of up to 6 percentage points in probability value of corrosion initiation and damage (or an equivalent 8% increase in a percentage term), and 0.9mm more mean rebar loss by 2100 for the three emission scenarios.

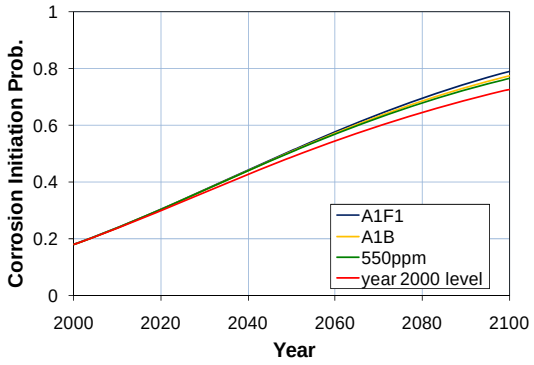

(a) Corrosion initiation probability

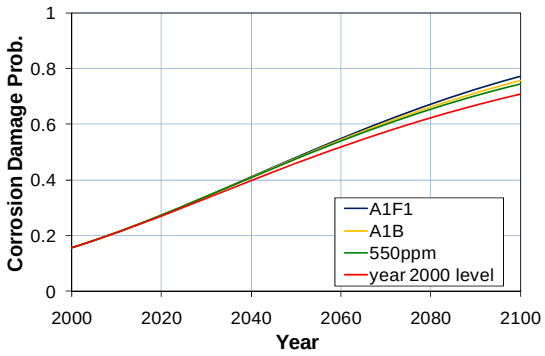

(b) Corrosion damage probability

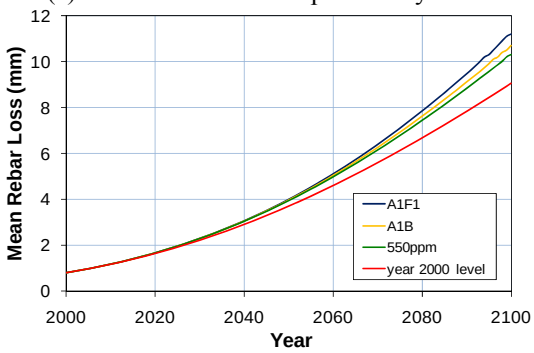

(c) Mean rebar loss (mm)

Figure 3-7 The probability of chloride-induced corrosion initiation and damage and mean rebar loss of Bridge BD1 in a temperate climate zone, with the effect of climate change in comparison with the baseline in the absence of climate change. 'year 2000 level' is the relevant value in the absence of climate change. (The probability is represented by decimal numbers)

3.1.3 1959-1970 Bridge Structures

Bridges BA2 (1959, Southern Region)

Bridge BA2 has been in service for 49 years to 2008 since constructed, as shown in Figure 3-8. The simulation based on the tests of concrete structures at a location with exposure C2 indicates that the probability of corrosion initiation and damage were almost equal to 100 percentage points or corrosion is almost certain by 2008. The impact of climate change was subdued as it would not be able to make too much difference on the corrosion (or make corrosion more severe). Therefore the climate change impact will not be discussed for this bridge.

Bridge BC2 (1968, Hunter Region)

Bridge BC2 in the Hunter region has been in service for 40 years to 2008 as shown in Figure 3-9, and appears severe corrosion at a location of bridge structures under exposure C2, in terms of the probability of corrosion initiation and damage for more than 90 percentage points in 2008. At such a degree of corrosion severity, there is only a very limited impact of climate change.

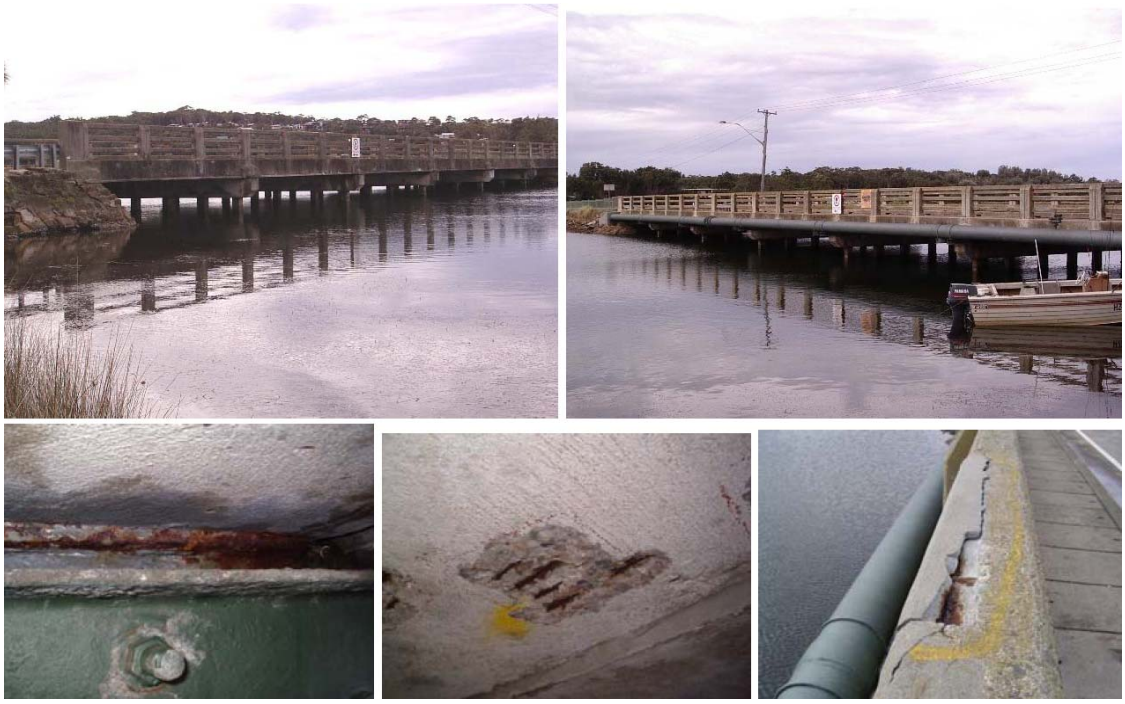

Figure 3-8 Bridge BA2 constructed in 1959 in the southern region of NSW (Source: RTA)

Figure 3-9 Bridge BC2 constructed in 1968 in Hunter region of NSW (Source: RTA)

As shown in Figure 3-10, by 2100, corrosion initiation and damage are almost certain, regardless of climate change that only causes no more than an 0.3 percentage points increase in probability. However, climate change is projected to cause up to 2.1mm increase of mean rebar loss by 2100, about an 10% increase of the rebar loss in the absence of climate change.

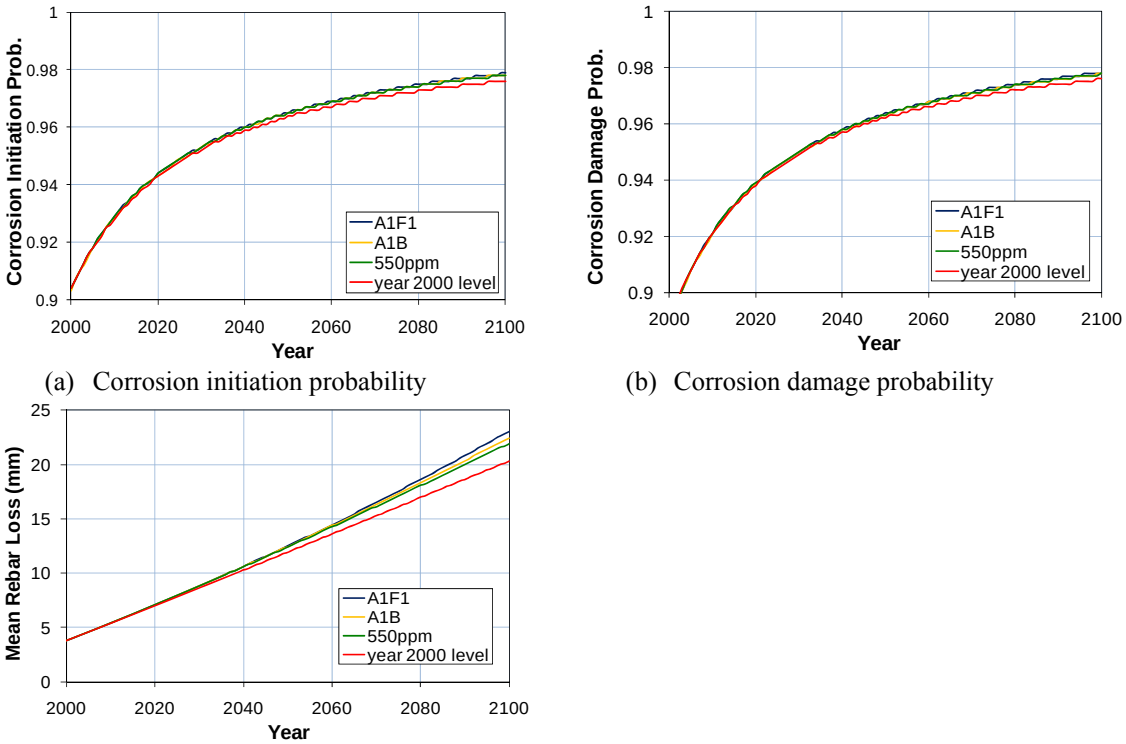

(a) Corrosion initiation probability

(b) Corrosion damage probability

(c) Mean rebar loss (mm)

Figure 3-10 The probability of chloride-induced corrosion initiation and damage and mean rebar loss of Bridge BC2 in a temperate climate zone, with the effect of climate change in comparison with the baseline in the absence of climate change. 'year 2000 level' is the relevant value in the absence of climate change. (The probability is represented by decimal numbers)

Bridge BD2 (1967, Northern Region)

Bridge BD2 in NSW has been in service for 41 years by 2008, as shown in Figure 3-11. The tested part of structures at a location with exposure C2 shows very low corrosion by 2008. It is represented by the low probability of corrosion initiation and damage that was estimated around 3 percentage points while the mean rebar loss was negligible.

As shown in Figure 3-12, by 2100, the probability of chloride-induced corrosion initiation is projected to be 46, 45 and 43 percentage points for A1FI, A1B and 550 ppm stabilisation emission scenario, respectively, in comparison with 39 percentage points in the absence of climate change. The probability of corrosion damage is projected to be 44, 43 and 42 percentage points for the three emission scenario in comparison with 38 percentage points in the absence of climate change. The mean rebar loss is 4.6mm, 4.2mm and 4.0mm by 2100 for the three emission scenarios in comparison 3.3mm in the absence of climate change.

Figure 3-11 Bridge BD2 constructed in 1967 in the northern region of NSW (Source: RTA)

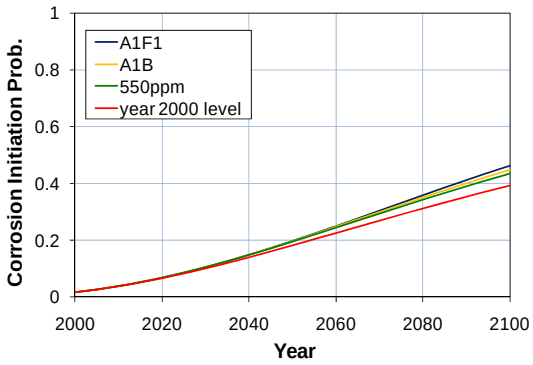

(a) Corrosion initiation probability

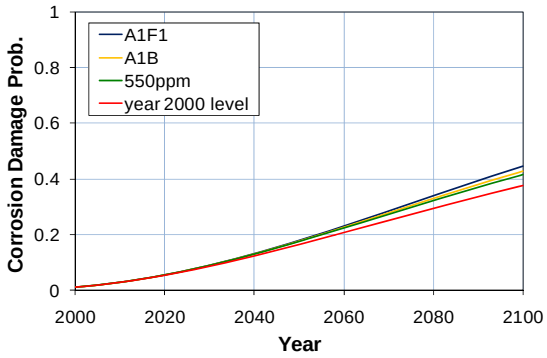

(b) Corrosion damage probability

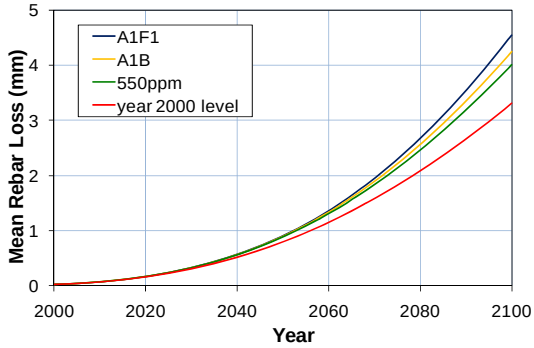

(c) Mean rebar loss (mm)

Figure 3-12 The probability of chloride-induced corrosion initiation and damage and mean rebar loss of Bridge BD2 in a temperate climate zone, with the effect of climate change in comparison with the baseline in the absence of climate change. 'year 2000 level' is the relevant value in the absence of climate change. (The probability is represented by decimal numbers)

In other words, climate change leads to an 7 percentage points increase in probability of corrosion initiation and damage (or an equivalent 18% increase in percentage change of corrosion initiation probability due to climate change). It also causes up to 1.2mm

increase in mean rebar loss (or 39% more than the mean rebar loss without the effect of climate change).

3.1.4 1971-1994 Bridge Structures

Bridge BA3 (1980, Southern Region)

Bridge BA3 in NSW has been in service for only 28 years by 2008, as shown in Figure 3-13, but structures under exposure C2 at a location shows certain corrosion initiation and corrosion damage with the mean rebar loss of 4.1mm. The effect of climate change on the corrosion initiation and damage of structures is minimal when the corrosion tends to be certain or almost certain. However, climate change is projected to increase the mean rebar loss by up to 2.8mm, or an equivalent increase of 14% in comparison with the mean rebar loss in the absence of climate change.

Figure 3-13 Bridge BA3 constructed in 1980, in the southern region of NSW (Source: RTA)

Bridge BC3 (1989, Hunter Region)

Bridge BC3 has been in service for 24 years by 2008, showing fairly small extent of corrosion with a negligible mean rebar loss while the probability of corrosion initiation

is at 3 percentage points , and the probability of corrosion damage is about 1 percentage points .

Figure 3-14 Bridge BC3 constructed in 1989 in the Hunter region of NSW (Source: RTA)

However, as shown in Figure 3-15, the probability of corrosion initiation and damage can increase dramatically after 2020, reaching to about 95% in 2060.

The effect of climate change increases the probability of corrosion initiation and damage by 4 percentage points more than those in the absence of climate change by 2045, and the relative effect decreases with the increase of the probability or corrosion severity. By 2100, the mean rebar loss is projected to be up to 2.8mm more than the loss in the absence of climate change, or an equivalent 24% increase.

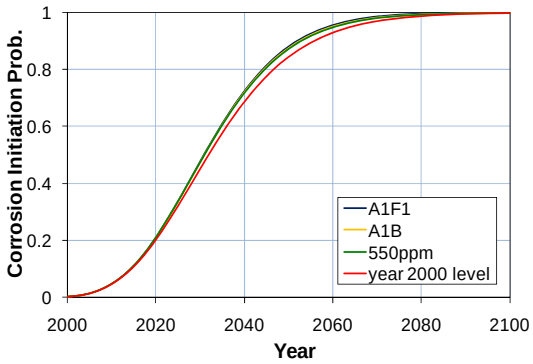

(a) Corrosion initiation probability

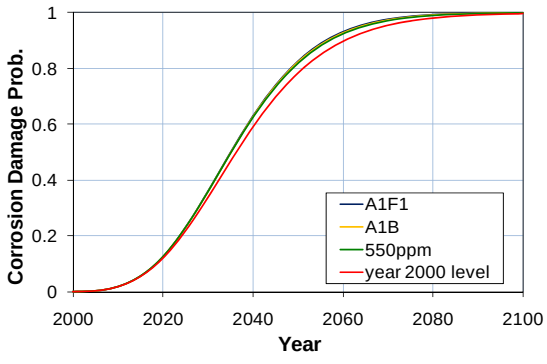

(b) Corrosion damage probability

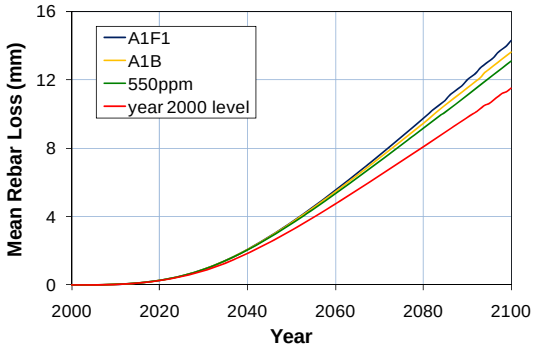

(c) Mean rebar loss (mm)

Figure 3-15 The probability of chloride-induced corrosion initiation and damage and mean rebar loss of Bridge BC3 in a temperate climate zone, with the effect of climate change in comparison with the baseline in the absence of climate change. 'year 2000 level' is the relevant value in the absence of climate change. (The probability is represented by decimal numbers)

Bridge BD3 (1984, Northern Region)

Bridge BD3 has been in service for 24 years by 2008 since constructed in 1984, as shown in Figure 3-16, and currently shows relatively low likelihood of corrosion at the a location of structures under exposure C1 as well at another location of structures under exposure C2. By 2008, the probability of corrosion initiation and damage as well as the mean rebar loss of concrete exposed to C1 were 6 and 2 percentage points with a negligible mean rebar loss, respectively. For that exposed to C2, the probability was all around 3% by 2008. As shown in Figure 3-17 and Figure 3-18, climate change may have noticeable impact on the probability as well as mean rebar loss.

Figure 3-16 Bridge BD3 constructed in 1984 in the northern region of NSW (Source: RTA)

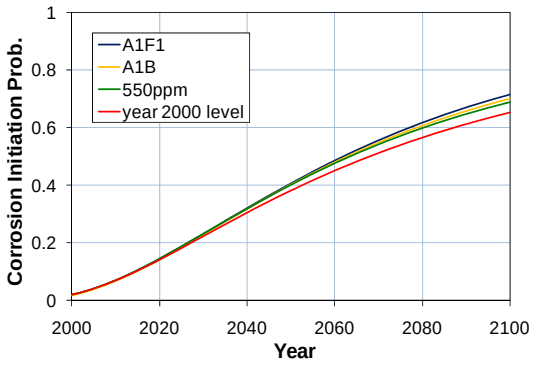

(a) Corrosion initiation probability

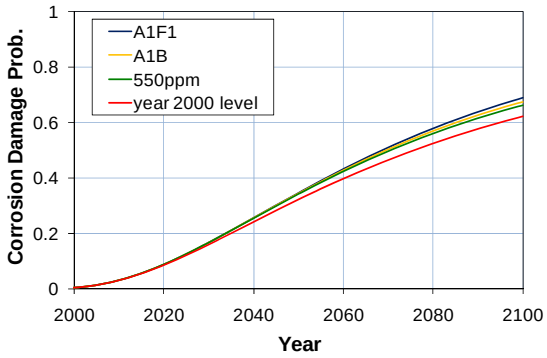

(b) Corrosion damage probability

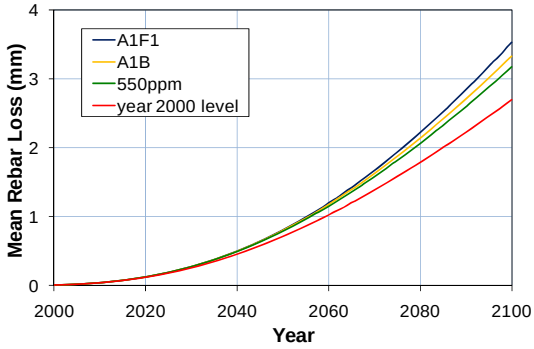

(c) Mean rebar loss (mm)

Figure 3-17 The probability of chloride-induced corrosion initiation and damage and mean rebar loss of concrete structures of Bridge BD3 at exposure C1 in a temperate climate zone, with the effect of climate change in comparison with the baseline in the absence of climate change. 'year 2000 level' is the relevant value in the absence of climate change. (The probability is represented by decimal numbers)

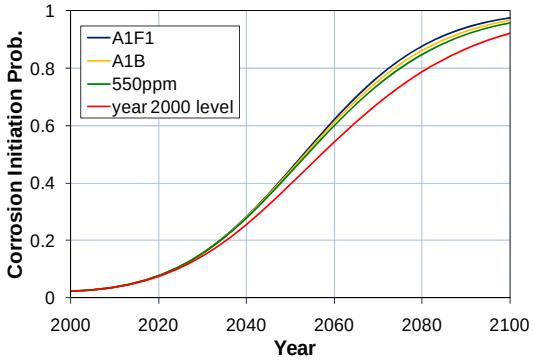

(a) Corrosion initiation probability

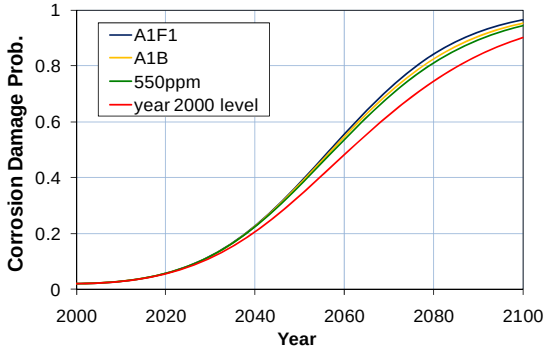

(b) Corrosion damage probability

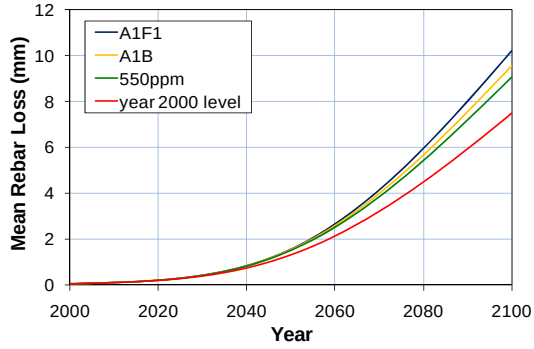

(c) Mean rebar loss (mm)

Figure 3-18 The probability of chloride-induced corrosion initiation and damage and mean rebar loss of concrete structures of Bridge BD3 at exposure C2 in a temperate climate zone, with the effect of climate change in comparison with the baseline in the absence of climate change. 'year 2000 level' is the relevant value in the absence of climate change. (The probability is represented by decimal numbers)

For the concrete structures of Bridge BD3 at exposure C1 under the effect of climate change, the probability of corrosion initiation is projected to be 72 percentage points for A1FI emission scenario, 70 percentage points for A1B emission scenario, and 69 percentage points for 550 ppm stabilisation emission scenario, in comparison with 65 percentage points projected in the absence of climate change by 2100. The probability of corrosion damage is projected to be 69, 67 and 66 percentage points for the three emission scenarios respectively in comparison with 62 percentage points projected without the effect of climate change. The mean rebar loss will be 3.5mm, 3.3mm and 3.2mm for the three emission scenarios respectively in comparison 2.7mm estimated in the absence of climate change. In other words, as a result of the climate change, the mean rebar loss may increase by 30%, 22% and 19%, respectively, in association with the emission scenarios.

For the concrete structures of Bridge BD3 at exposure C2 under the effect of climate change, the probability of corrosion initiation is projected to be up to 9 percentage points more than the probability projected in the absence of climate change by 2070 (or an equivalent13% increase in a percentage term). The probability of corrosion damage is up to 10 percentage points more by 2075 (or an equivalent 14% increase in a percentage term). The impact of climate change on the probability value increase is reduced to 5-6 percentage points by 2100 (or an equivalent 6-7% increase in a percentage term). In addition, the mean rebar loss will be 10.2mm, 9.6mm and 9.1mm for the three emission scenarios respectively in comparison with 7.5mm by 2100 in the absence of climate change, indicating 36%, 28% and 21% increases in rebar loss. It appears that the impact of climate change is more on concrete at exposure C2 than C1.

3.2 Carbonation-Induced Corrosion of Concrete Bridges

3.2.1 Bridges for Carbonation-Induced Corrosion Assessment

Seven bridges exposed to C1 and C2 in the temperate climate zone in NSW, as shown in Table 3-2, are applied for the assessment of likely impact of climate change. Similar to those bridges for the case study of chloride-induced corrosion, the bridges are divided into four regions, i.e. Southern, Sydney, Hunter and Northern region, and four construction periods, i.e. pre-1959, 1959-1970, 1971-1994 and post-1995. The field carbonation test data was provided with a range of carbonation depth (CR) listed in the Table. However, they are not available for all bridges. The assessment will be done only for those with available carbonation depth information.

Table 3-2. List of bridges assessed for carbonation-induced corrosion

Construction Period	Region			
	Southern	Sydney	Hunter	Northern
Pre-1959	**Bridge BA1** 1956 CR: 10 – 25 mm Cover: 55mm	**Bridge BB1** 1925 CR: 5 – 35 mm Cover: 29mm	*Test data not available*	*Test data not available*
1959 – 1970	**Bridge BA2** 1959 CR: 1 – 5 mm Cover: 50mm	**Bridge BB2** 1959 CR: 5 – 15 mm Cover: 48mm	**Bridge BC2** 1968 CR: 5 – 25 mm Cover: 53mm	*Test data not available*
1971 – 1994	**Bridge BA3** 1980 CR: 5 – 20 mm Cover: 58mm	*Test data not available*	*Test data not available*	**Bridge BD3** 1984 CR: 2 – 10 mm Cover: 62mm
Post-1995	*Test data not available*	*Test data not available*	*Test data not available*	*Test data not available*

3.2.2 Pre-1959 Bridge Structures

Bridge BA1 (1956, Southern Region)

Bridge BA1 was built in 1956. Concrete in the test site has cover of 55mm with exposure C1-C2. The mean carbonation depth in 2008 is 17.5mm as tested. As shown in Figure 3-19, climate change may have noticeable impact on the carbonation depth. By 2100, the mean carbonation depth is 34.0mm for A1FI emission scenario, 31.9mm for A1B emission scenario, and 30.1mm for 550ppm stabilisation scenario in comparison with 26.5mm estimated in the absence of climate change, or 28% 20% and 14% more, respectively. However, 55mm cover of concrete has almost prevented the occurrence of corrosion initiation and damage represented by their negligible probability along with a very small mean rebar loss, even if climate change would contribute a significant increase in carbonation depth. On the other hand, it demonstrated the importance of proper cover design to reduce the impact of carbonation on corrosion of reinforcement.

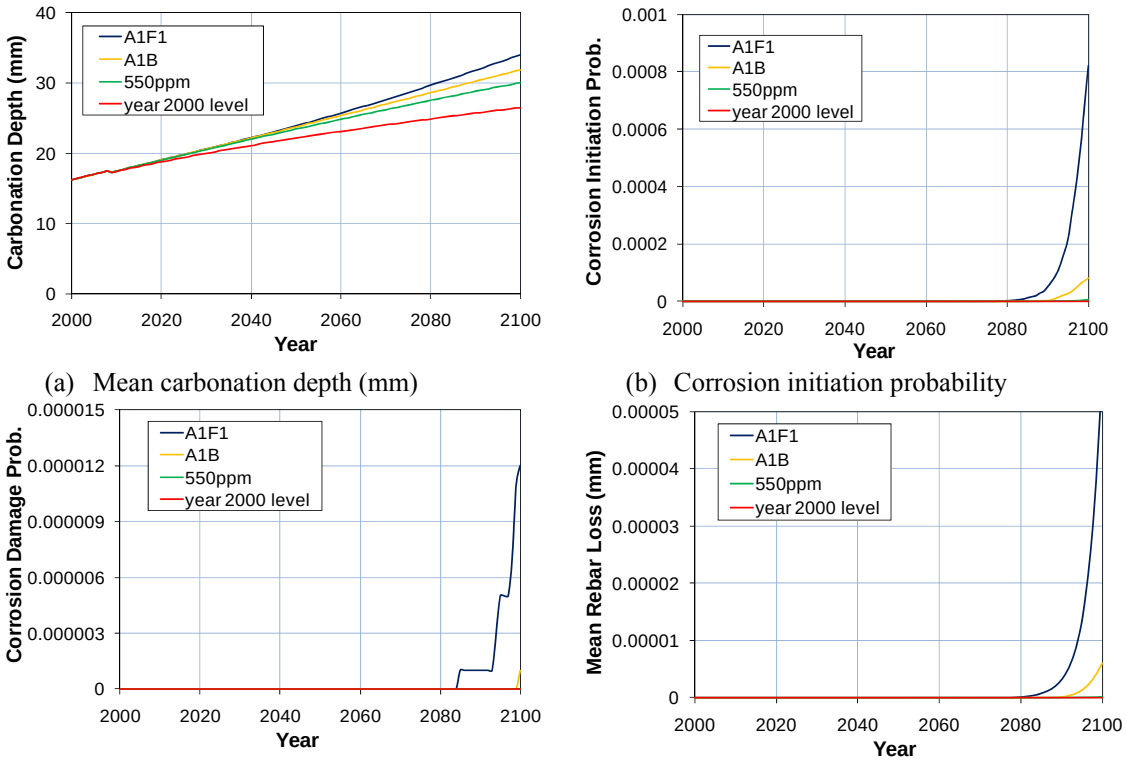

(a) Mean carbonation depth (mm)

(b) Corrosion initiation probability

(c) Corrosion damage probability

(d) Mean rebar loss (mm)

Figure 3-19 Carbonation depth, probability of carbonation-induced corrosion initiation and damage and mean rebar loss of concrete structures of Bridge BA1 in a temperate climate zone, with the effect of climate change in comparison with the baseline in the absence of climate change. 'Year 2000 level' is the relevant value in the absence of climate change. (The probability is represented by decimal numbers)

Bridge BB1 (1925, Sydney)

The part of structures of Bridge BB1 built in 1925 has a concrete cover of 29mm. Field tests found carbonation in the range of 5-35mm, very likely inducing corrosion. As shown in Figure 3-20, the mean carbonation depth is 35.2mm for A1FI emission scenario, 33.3mm for A1B emission scenario, and 31.6 for 550ppm stabilisation emission scenario by 2100, in comparison with 28.4mm estimated without the effect of climate change.

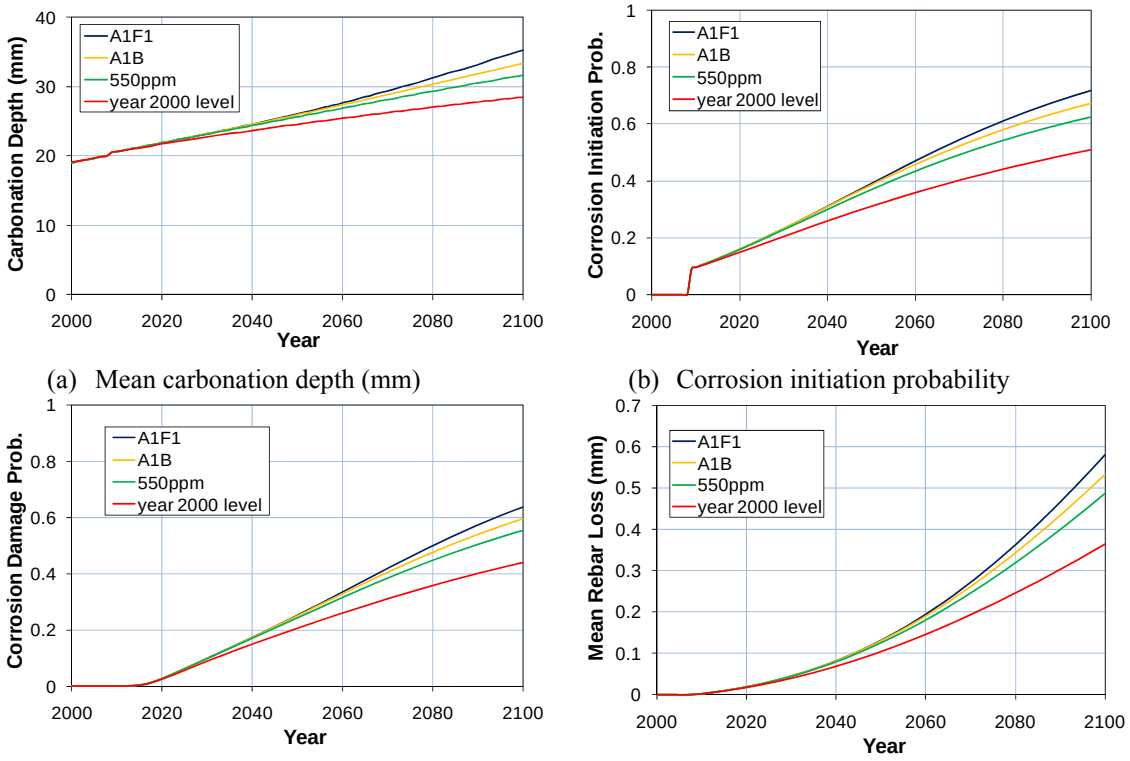

(a) Mean carbonation depth (mm)

(b) Corrosion initiation probability

(c) Corrosion damage probability

(d) Mean rebar loss (mm)

Figure 3-20 Carbonation depth, probability of carbonation-induced corrosion initiation and damage and mean rebar loss of concrete structures of Bridge BB1(1925) in a temperate climate zone, with the effect of climate change in comparison with the baseline in the absence of climate change. 'year 2000 level' is the relevant value in the absence of climate change. (The probability is represented by decimal numbers)

As carbonation at the mean depth of 28.4mm in the absence of climate change is already very close to cover thickness of 29mm, any increase in carbonation depth caused by climate change may significantly impact on the probability of corrosion initiation and damage. As shown in Figure 3-20, the probability of corrosion initiation is 72, 67 and 63 percentage points for the three emission scenarios respectively in comparison with 51% estimated in the absence of climate change. In other words, the probability increases 21%, 16% and 12% percentage points in probability, or an equivalent increase of 41%, 31% and 14% in a percentage term due to climate change. Meanwhile, the probability of corrosion damage is 63, 60 and 55 percentage points in comparison with 44 percentage points estimated in the absence of climate change.

3.2.3 1959-1970 Bridge Structures

Bridge BA2 (1959, Southern Region)

Bridge BA2 was constructed in 1950. The concrete in the test site has 50mm cover. The carbonation depth was identified in the range of 1-5mm, which is much less than the cover thickness. Therefore, the likelihood of carbonation-induced corrosion is very low, and the impact of climate change is unlikely to alter the likelihood substantially though it may affect the carbonation depth as discussed previously.

Bridge BB2 (1959, Sydney)

Bridge BB2, constructed in 1959, has cover of 48mm, and the carbonation depth was tested in the range of 5-15mm that is much less than the cover. In this regard, the impact of climate change has little significance on corrosion initiation and damage, though the mean carbonation depth is projected to increase. The projected mean carbonation depth reaches 19.8mm for A1FI emission scenario, 18.6 for A1B emission scenario, and 17.5mm for 550 stabilisation scenario by 2100, in comparison with 15.4mm estimated without the effect of climate change, but they are far less than the cover thickness to reach the reinforcement.

Bridge BC2 (1968, Hunter Region)

Bridge BC2 was constructed in 1968. The reinforced concrete at test site has 53mm cover with carbonation measured in the range of 5-25mm. The carbonation depth is still far less than the level that can induce corrosion of reinforcement. Climate change may affect the carbonation depth, but is unlikely to have an influence on the probability of corrosion initiation and damage. The carbonation depth is projected to be 32.2mm, 30.1mm and 28.3mm by 2100 for the three emission scenarios in comparison with 24.7mm in the absence of climate change.

3.2.4 1971-1994 Bridge Structures

Bridge BA3 was constructed in 1980 and Bridge BD3 was constructed in 1984. The concrete cover at test site is 58mm and 62mm, respectively. The measured carbonation depth is much smaller than the cover, implying that there is less significance in the occurrence of carbonation-induced corrosion.

Strengthened concrete piles of port structures (source: CSIRO)

4. CLIMATE CHANGE IMPACT ON CORROSION OF EXISTING CONCRETE PORT STRUCTURES IN TROPICAL CLIMATE ZONES

Concrete structures, including a slab soffit and a column in a berth of Port Townsville, Queensland, as shown in Figure 4-1, are considered for the case studies.

The berth was constructed circa 1960. It consists of a flat reinforced concrete deck approximately 530 mm thick, supported by circular reinforced concrete columns, as shown in Figure 4-2 (or the head photo of this chapter), generally 760 mm in diameter, with some 910 mm in diameter, on a 6.1 m square grid which are founded on pile caps which are in turn supported by driven universal piles. The berth and its adjacent have been constructed as a single rectangular wharf structure with the central portion of the concrete structure founded of fill. They appear to comprise the same reinforced concrete retaining walls, piles and slabs that extend around three sides of the wharf. The total wharf structure is approximately 250 m long and 70 m wide with the piled area for each berth is approximately 22m wide.

Following detailed inspections in 2008, the reinforced concrete of the berth is in a relatively good condition considering its age of 50 years (48 years in 2008). The results of the 2008 condition assessment indicated that with ongoing inspection and maintenance the deck should be serviceable for the next 50 years. The support columns for the berth were at risk of widespread deterioration within the next 10 years and are currently undergoing remedial works.

Figure 4-1 View of Port Townsville and its berths by Google Map

The test was done in 37 locations of the slab soffit with a cover of 50mm, and 8 locations of columns with a cover of 60mm. The test data of chloride concentration profiles and carbonation depth were provided by Port of Townsville, (2009). While chloride-induced corrosion is assessed on the location of slab soffits or columns with the highest chloride concentration, the carbonation-induced corrosion is assessed on the whole structures of the berth with different carbonation depths considered as an uncertainty in carbonation.

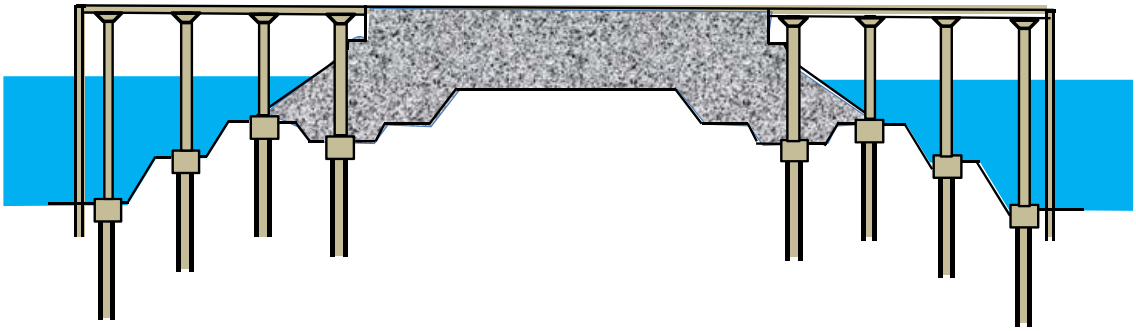

Figure 4-2 Concrete slabs and columns of the Berth

4.1 Chloride-Induced Corrosion of Port Structures

Slab Soffits

The tests were done for the concrete slab soffit between column 33 and 34 at column line N of the berth in Port Townsville in 2008. The slab has a cover of 50mm and is considered under exposure C2. The chloride content analysis shows the chloride concentration at 0.32%, 0.21%, 0.12% and 0.04 % by weight of concrete in the depth of 5mm, 20mm, 40mm and 50mm, respectively. With the concentration profile, the probability of chloride-induced corrosion initiation and damage is estimated at 10% and 9%, respectively, and likely mean rebar loss at 0.34mm by 2008.

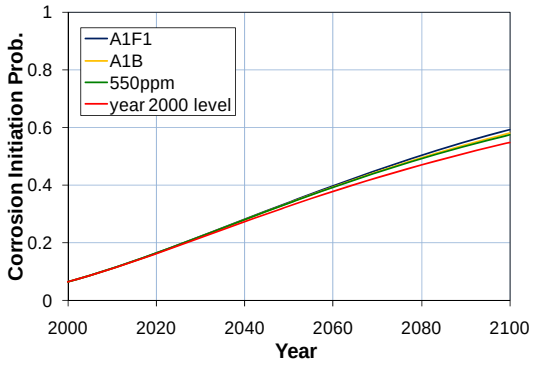

(a) Corrosion initiation probability

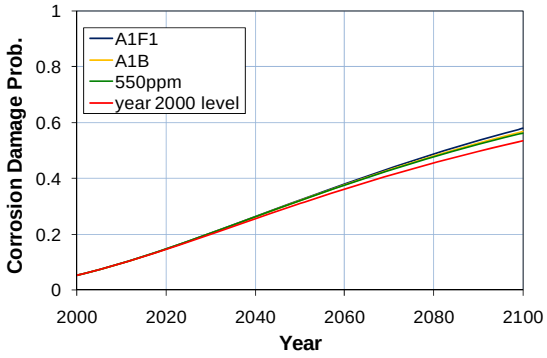

(b) Corrosion damage probability

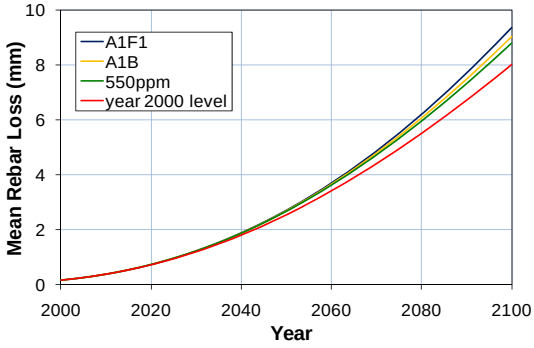

(c) Mean rebar loss (mm)

Figure 4-3 Probability of chloride-induced corrosion initiation and damage and mean rebar loss of concrete structures of a slab soffit (33-34N) in a tropical climate zone, with the effect of climate change in comparison with the baseline in the absence of climate change. 'Year 2000 level' is the relevant value in the absence of climate change. (The probability is represented by decimal numbers)

As shown in Figure 4-3, the probability of corrosion initiation is projected to reach 59 percentage points by 2100 for A1FI emission scenario, 58 percentage points for A1B emission scenario and 57 percentage points for 550ppm stabilisation emission scenario in comparison with 55 percentage points in the absence of climate change. The probability of corrosion damage is 58, 57 and 56 percentage points for the three emission scenarios respectively in comparison with 54 percentage points estimated without the effect of climate change. The mean rebar loss is project to be 9.3mm, 9mm

and 8.8mm for three emission scenarios in comparison with 8mm without the effect of climate change.

In this regard, the impact of climate change by 2100 is limited within a 4 percentage points increase in probability of corrosion initiation and damage (or an equivalent increase of 7.4% in a percentage term), and it is within 1.3mm of mean rebar loss or a increase of 16%.

Columns

Column L5 of the berth in Port Townsville is selected as the case study of concrete port structures. It has cover of 60mm. The core sample from the column for chloride concentration analysis is located 500mm below tapered section of the column, and is considered at exposure C2. The chloride concentration analysis was done in 2008 and details the concentration profile that is 0.28%, 0.1%, 0.04%, 0% by the weight of concrete at the depth of 5mm, 20mm, 40mm and 60mm, respectively. Based on the chloride concentration profile, the probability of corrosion initiation and damage is less than 1% by 2008 and the mean rebar loss is estimated at 0.024mm.

As shown in Figure 4-4, the probability of corrosion of initiation and damage is projected less than 1.2% for all emission scenarios by 2100. The significance of climate change impact is very limited.

4.2 Carbonation-Induced Corrosion of Port Structures

Slab Soffits

The tests were done at 37 locations for the concrete slab soffit of the berth in Port Townsville in 2008. The slab has a cover of 50mm. The test of core sample from the slab shows carbonation depth in the range of 22mm to 55mm in 2008. On the basis of the test, it seems that there would be any occurrence of carbonation-induced corrosion initiation and damage by 2008.

As shown in Figure 4-5, the probability of corrosion initiation and damage as well as mean rebar loss may increase significantly over the years, and climate change may even magnify the change.

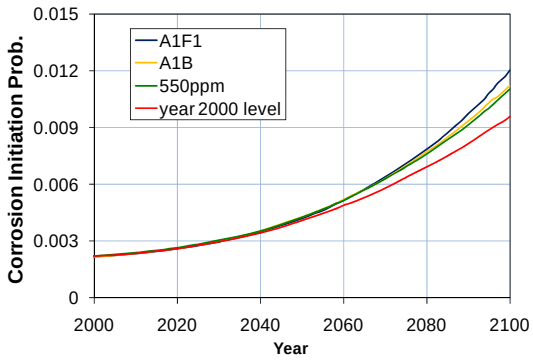

(a) Corrosion initiation probability

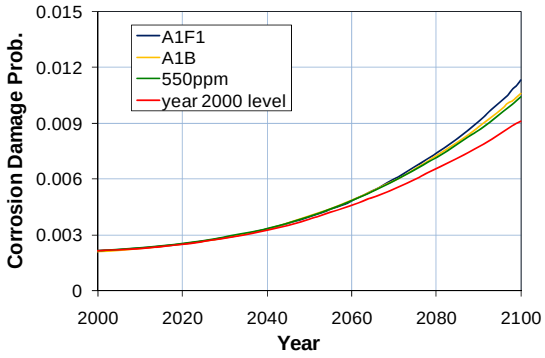

(b) Corrosion damage probability

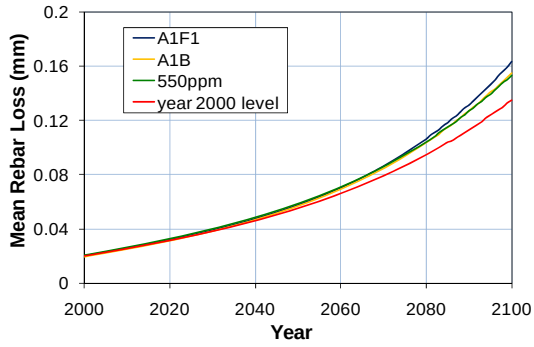

(c) Mean rebar loss (mm)

Figure 4-4 Probability of chloride-induced corrosion initiation and damage and mean rebar loss of concrete structures of column (L5) in a tropical climate zone, with the effect of climate change in comparison with the baseline in the absence of climate change. 'Year 2000 level' is the relevant value in the absence of climate change. (The probability is represented by decimal numbers)

As seen in the figure, by 2100, the probability of carbonation-induced corrosion initiation is projected to reach 91 percentage points for A1FI emission scenario, 89 percentage points for A1B emission scenario, and 86 percentage points for 550 ppm stabilisation emission scenario in comparison with 76 percentage points in the absence of climate change. In other words, climate change causes 15, 13 and 10 percentage points increase in probability. In the term of percentage change, an equivalent increase of 20%, 17% and 13% in percentage terms, respectively. In fact, climate change leads to the largest impact on the probability of corrosion initiation around 2080, where the probability is 16 percentage points more than one estimated without the effect of climate change, or an increase of 31% in the term of percentage change.

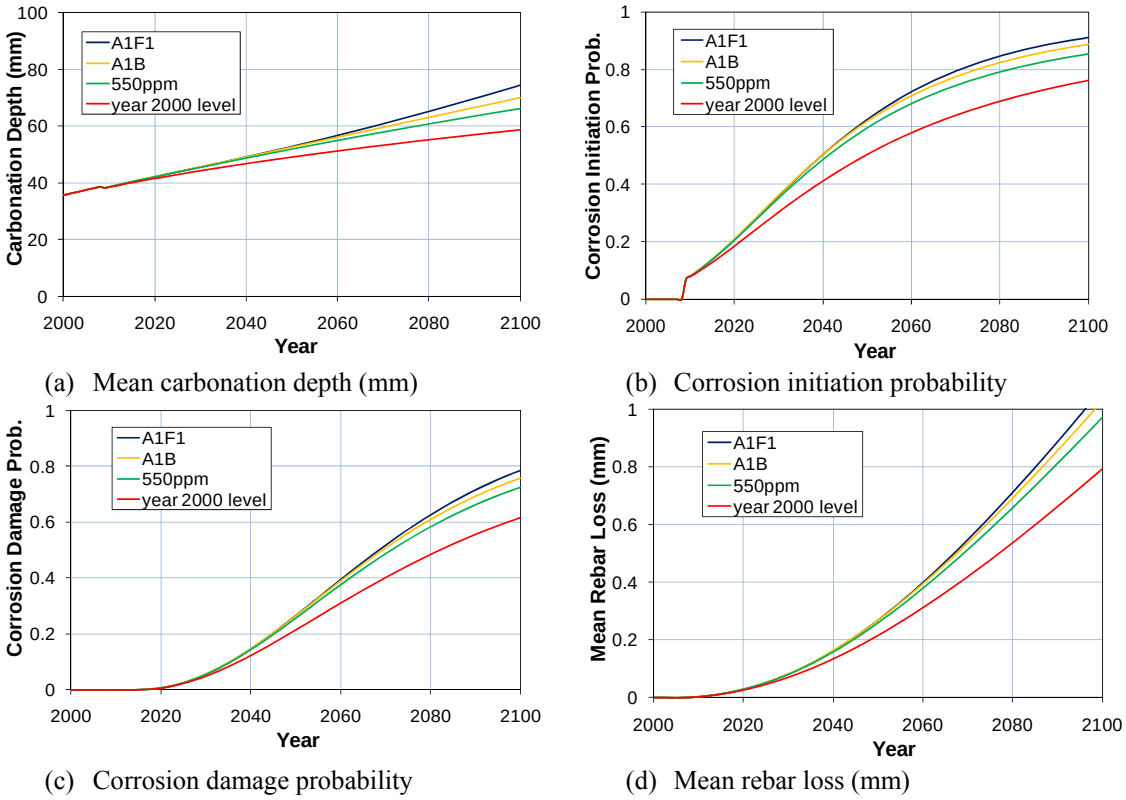

(a) Mean carbonation depth (mm)

(b) Corrosion initiation probability

(c) Corrosion damage probability

(d) Mean rebar loss (mm)

Figure 4-5 Carbonation depth, probability of carbonation-induced corrosion initiation and damage and mean rebar loss of concrete structures of a column Slab soffits in a tropical climate zone, with the effect of climate change in comparison with the baseline in the absence of climate change. 'Year 2000 level' is the relevant value in the absence of climate change. (The probability is represented by decimal numbers)

Meanwhile, the probability of corrosion damage is 78, 76 and 73 percentage points by 2100 for the three emission scenario, respectively, in comparison with 62 percentage points in the absence of climate change. In the term of percentage change, it is an increase of 26%, 23% and 18%, respectively. The mean rebar loss is 1.1mm, 1.0mm, 0.97mm for the three emission scenario in comparison with 0.79mm estimated without the effect of climate change.

Columns

Columns of the berth have a cover of 60mm. The core samples of the column were taken from 7 locations for carbonation depth assessment. The samples are located 500mm below tapered section of the column, showing a carbonation depth in the range of 22mm to 38mm by 2008. At such a depth of carbonation, it is very unlikely that the carbonation would cause any corrosion initiation and damage. As shown in Figure 4-6, without the effect of climate change, the carbonation depth is projected to reach 46.1mm by 2100. Although it is approaching the end of cover (60mm), it would still not cause significant change in the probability of corrosion initiation and damage.

As shown in the figure, the consideration of climate change significantly increases the probability of carbonation-induced corrosion, especially after 2060 for corrosion initiation and 2070 for corrosion damage. The probability of corrosion initiation is 45 percentage points for A1FI emission scenario, 28 percentage points for A1B emission scenario and 14 percentage points for 550 ppm stabilisation emission scenario, in comparison with only 1 percentage points in the absence of climate change. The probability of corrosion damage is projected to be 16, 8.8 and 4.0 percentage points for the three emission scenarios in comparison with 0.17 percentage points estimated without the effect of climate change.

As a result, in this case, the climate change may have considerable impact on the reliability of concrete port structures. It is noted that the design of concrete cover is very critical to prevent or reduce the impact of climate change.

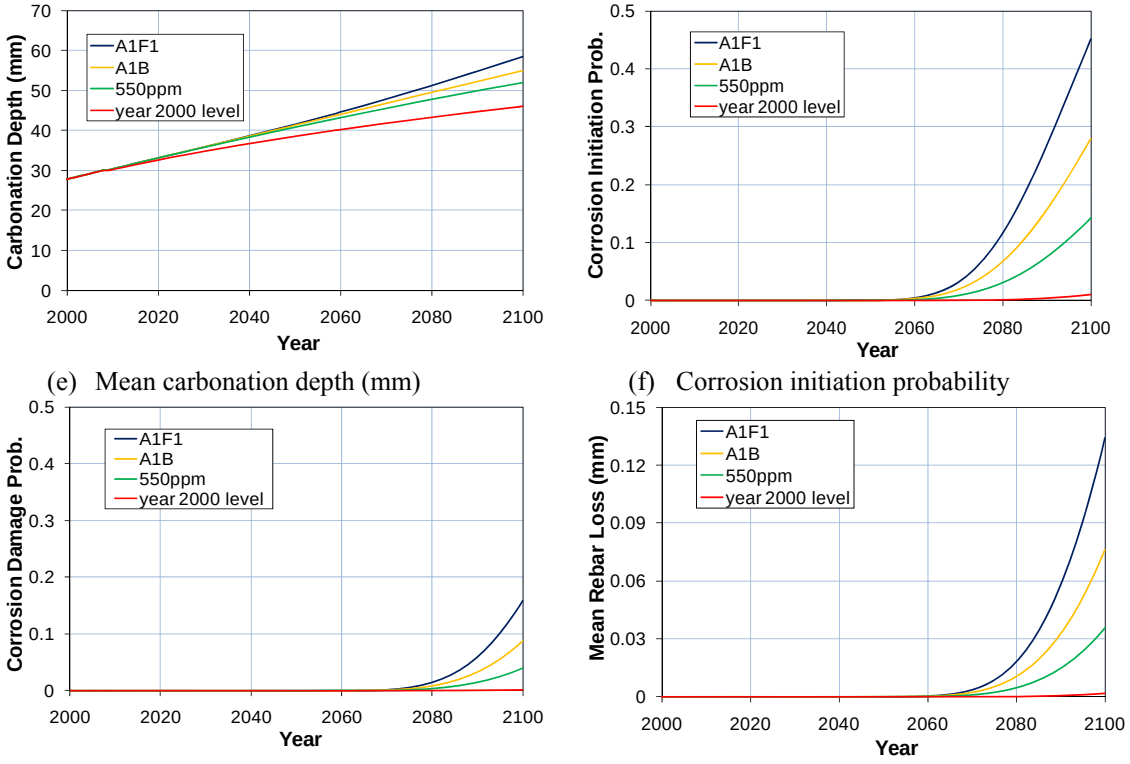

(e) Mean carbonation depth (mm)

(f) Corrosion initiation probability

(g) Corrosion damage probability

(h) Mean rebar loss (mm)

Figure 4-6 Carbonation depth, probability of carbonation-induced corrosion initiation and damage and mean rebar loss of concrete structures of a column (L5) in a tropical climate zone, with the effect of climate change in comparison with the baseline in the absence of climate change. 'Year 2000 level' is the relevant value in the absence of climate change. (The probability is represented by decimal numbers)

Adaptation measures to reduce deterioration (source: CSIRO and RTA)

5. ADAPTATION MEASURES TO COUNTERACT CLIMATE CHANGE IMPACT

Climate adaptation is considered as a process of deliberate change in anticipation of or in reaction to climatic stimuli and stress, in order to moderate or reduce adverse effects onto the system of our interest (IPCC, 2007). The critical component in climate adaptation is the adaptive capacity that measures the capability of the system to maintain its functionality and integrity under the disturbance of external stimuli and stresses. Enhancement of climate adaptive capacity, along with reducing vulnerability, is considered as one of prime approaches to counteract the changing climate.

For existing concrete structures under changing climate, the climate adaptation in terms of the enhancement of adaptive capacity can be done by developing new technologies for maintenance to counter the impact of increasing corrosion risk under changing climate. On the other hand, there is a wide range of conventional maintenance and retrofitting options that can enhance the durability of concrete structures and these can be applied to reduce the adverse affects of climate change. The maintenance options generally include surface coating, realkalisation, chloride extraction, cathodic protection, and cover replacement.

Creating a surface barrier by coating is more appropriate for reducing the exposure of concrete structure to external stimuli. Meanwhile, extraction and cathodic protection is more commonly carried out for structures with high corrosion risk to reduce the ingress of deleterious agents. The cover replacement is most effective, but also the most expensive option, followed by cathodic protection that also has operating cost and then

realkanisation or chloride extraction. The surface coating is the cheapest option, but is also less effective.

5.1 Simulation of Adaptation Measures for Chloride- and Carbonation-Induced Corrosion

To consider the worst scenario of climate change impact, A1FI emission scenario is applied to assess the adaptation of concrete structures for chloride-induced corrosion. Meanwhile, as indicated previously, the simulation of adaptation measures for chloride- and carbonation-induced corrosion is represented by various factors.

It is assumed in the simulation of adaptation measures for chloride-induced corrosion:

(1)Electrochemical Chloride Extraction 90%: correction factor for chloride concentration $R_{Chloride} = 0.1$, and correction factor for corrosion rate $R_{icorr} = 0.1$ accordingly. The cost is about \$600/m^2. It is a permanent solution if a surface coating is applied and properly maintained.

(2)Polyurethane sealer: It is able to reduce chloride diffusion coefficient. The estimation of diffusion coefficient is described in section 2.4.2, and relevant data described in Table 2-2. The cost is about \$40/m^2. The coating is applied every 15 years.

(3)Polymer-modified (p-m) cementious coating: it is able to reduce chloride diffusion coefficient. The estimation of diffusion coefficient is described in section 2.4.2, and relevant data described in Table 2-2. The cost is about \$40/m^2. The coating is applied every 15 years.

(4)Replacing existing cover: the new cover conforms to current concrete standards, as described in section 2.4.5. The cost is about \$2,500/m^2.

(5)Cathodic protection: it permanently stops corrosion initiation and damage. The cost includes \$800/m^2 initial cost and \$10/m^2/year operating cost.

At the same time, it is assumed in the simulation of adaptation measure for carbonation-induced corrosion:

(6)Realkalisation: It is a permanent solution if a surface coating is applied and properly maintained. The cost is about \$600/m^2.

(7)Acrylic-based coating: It is able to reduce carbonation diffusion coefficient. The estimation of diffusion coefficient is described in section 2.4.2, and relevant data described in Table 2-2. The cost is about \$50/m^2. The coating is applied every 15 years.

(8)Replacing existing cover: the new cover conforms to current concrete standards, as described in section 2.4.5. The cost is about \$2,500/m^2.

Adaptation measures are assumed to be applied in 2011 in the simulation (with some adaptation measures applied at regular intervals during the service life of the structure), and all cost is the present value in 2010.

5.2 Cost/Benefit Assessment of Adaptation Options

For adaptation measures, the residual risk is defined by:

$$\mathrm{Risk}(T) = \sum_{i=1}^{T/\Delta t} \frac{p_s(i\Delta t) - p_s([i-1]\Delta t)}{1 - p_s([i-1]\Delta t)} \tag{5-1}$$

where $p_s(i\Delta t)$ is the cumulative probability of corrosion damage at time $i\Delta t$ ($i=1,T/\Delta t$), and T is the service life. Since there is lack of information of damage cost, a proxy of the benefit due to the implementation of adaptation options in changing climate is defined by:

$$\text{Benefit} = \text{Risk}(T, \text{BAU} \mid \text{CC}) - \text{Risk}(T, \text{Adaptation} \mid \text{CC}) \tag{5-2}$$

where Risk(T, BAU | CC) is the risk in the circumstance of 'business as usual' or 'do-nothing' under climate change, and Risk(T, Adaptation | CC) is the residual risk after the implementation of an adaptation option under climate change. CC represents the effect climate change, and NCC represents no climate change considered.

Eqn.(5-2) can be rewritten as:

$$\text{Benefit} = \text{Benfit1} + \text{Benefit 2} - \text{Loss1} \tag{5-3}$$

where

Benefit 1 = Risk(T, BAU | CC)- Risk (T, BAU | NCC)
Benefit 2 = Risk (T, BAU | NCC)] - Risk(T, Adaptation | NCC)
Loss1 = Risk(T, Adaptation | CC) - Risk(T, Adaptation | NCC)

In Eqn. (5-3), the first term represents the benefit contributed by an adaptation option to mitigate the risk of corrosion completely due to climate change, the second term gives the benefit to increase corrosion resistance or adaptive capacity by the maintenance in the absence of climate change (the maintenance option is the same as adaptation option, applied to mitigate corrosion risk as usual but nothing to do with climate change), and the third term describes the loss of the benefit due to the reduced effectiveness of the adaptation option as a result of climate change. In another word, the cost is to offset the loss of effectiveness of adaptation options due to climate change.

Meanwhile, the adaptation cost is estimated on the basis of initial and operating cost to maintain the performance or function of adaptation measures given a discount rate.

In addition, 'Benefit' as described in Eqn.(5-3) also represents the degree of the reduction of corrosion risk when an adaptation option is applied, and can thus be considered as the representation of adaptation effectiveness. An option is not recommend when 'Benefit≤0'. The maximum benefit or adaptation effectiveness can be achieved when the risk, or Risk(T, Adaptation | CC) in Eqn.(5-1), approaches zero after an adaptation option implemented. However, this approach does not consider the cost-effectiveness of the 'business as usual' or 'do nothing' strategy. For this to be assessed would require a more formal life-cycle cost analysis.

Meanwhile, based on the cost and the effectiveness, an adaptation effectiveness diagram, such as shown in Figure 5-1, can be established to inform decision-makers to select proper adaptation options based on both effectiveness and cost. In the diagram, each bar represents an adaptation option with its width representing adaptation effectiveness and height representing cost. The optimal option is low cost and great effectiveness.

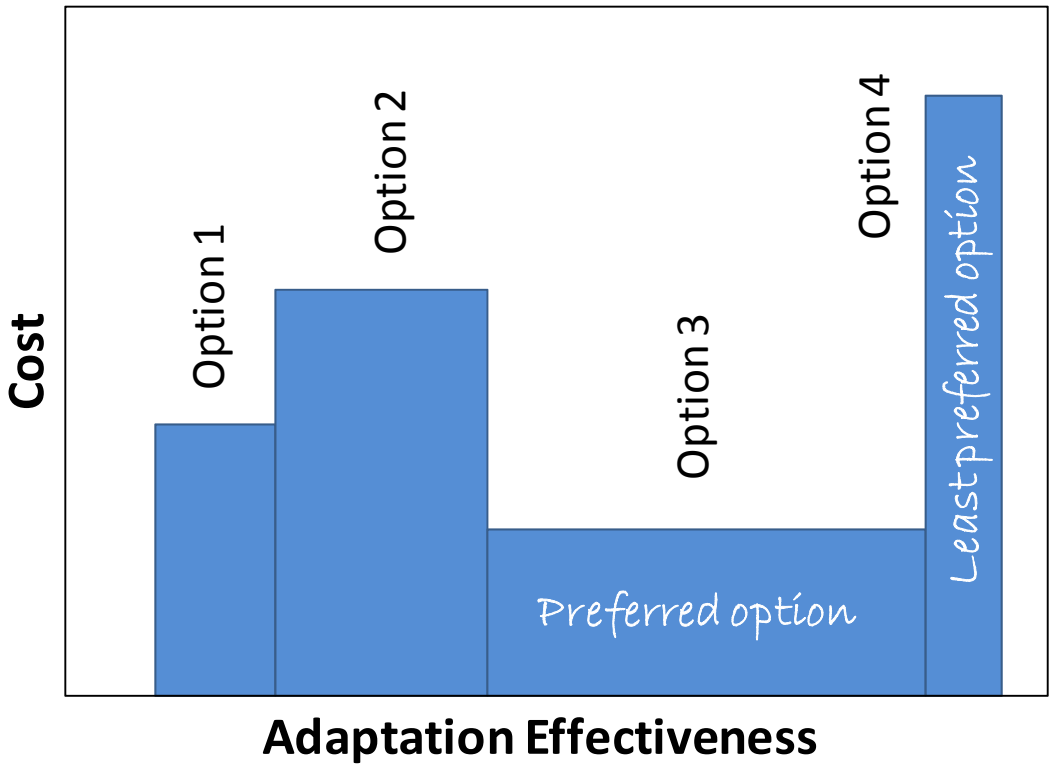

Figure 5-1 Conceptual illustration of adaptation effectiveness diagram

5.3 Adaptation Assessment for Chloride-Induced Corrosion and Cost/Benefit

5.3.1 Bridge BB1 Constructed in 1925 in Sydney

Figure 5-2 describes the effect of adaptation measures (1)-(4) described above on the probability of corrosion initiation and damage as well as rebar loss. It appears the most effective approach is the replacement of old 29mm cover of concrete with new concrete that meets the current design stands of 65mm cover at exposure C2. The measure not only counteract the impact of climate change, but also enough to maintain the probability of corrosion initiation and damage at a very low level and almost no further rebar loss.

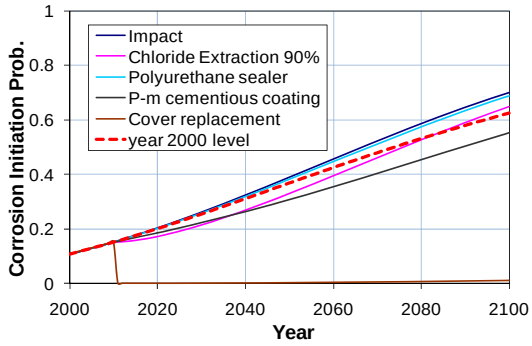

(a) Corrosion initiation probability

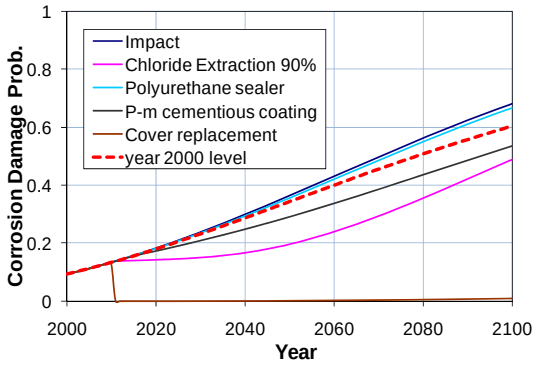

(b) Corrosion damage probability

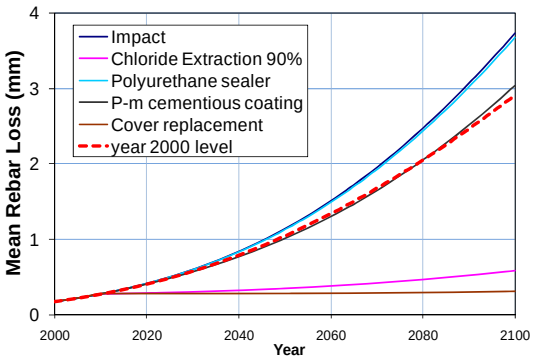

(c) Mean rebar loss (mm)

Figure 5-2 Probability of chloride-induced corrosion initiation and damage and mean rebar loss of concrete structures of Bridge BB1 (1925) in NSW considering adaptation options (1)-(4). 'Impact' - with the effect of climate change; 'Year 2000 level' – the relevant value in the absence of climate change. (The probability is represented by decimal numbers)

The second most effective approach is chloride extraction that assumes that 90% of chloride was removed. Although it is still projected that there is an increase in the probability of corrosion initiation and damage, but it maintain the probability of corrosion initiation below the estimation in the absence of climate change until 2080, and maintain the probability of corrosion damage below the projection in the absence of climate change. In another word, it has at least mitigated the impact of climate change.

The use of p-m cementious coating may also maintain the probability of corrosion initiation and damage below the estimation in the absence of climate change, while relatively less effective. In addition, polyurethane sealer, as indicated in Table 2-2, has little effect on the probability and mean rebar loss, and is thus not recommended for use.

Considering a service life of concrete structure till 2100, the cost (in AU$) and cost/benefit ratio is shown in Figure 5-3. It should be pointed out that the cost/benefit ratio is not in the sense of the ratio of dollar to dollar, and it is just a relative indicator for the comparison. As shown in the figure, cover replacement is most expansive and also very high in cost/benefit ratio among the five options, while p-m cementious coating is the least. The cost/benefit ratio of the implementation of polyurethane sealer is most sensitive to the discount rate.

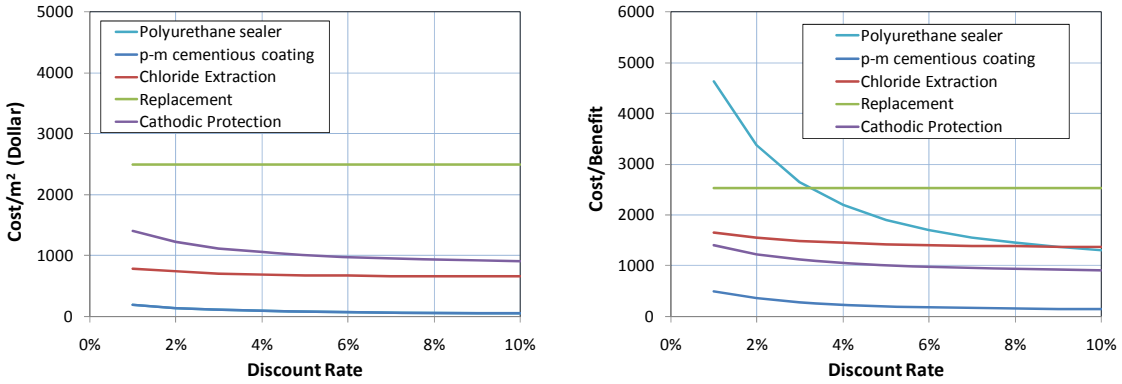

(a) Cost (b) Cost/Benefit

Figure 5-3 Cost (AU$) and cost/benefit ratio in relation to discount rate for the implementation of adaptation options for chloride-induced corrosion of concrete structures of Endeavour Bridge (1925) in NSW under climate change.

The cost is contributed to reduce corrosion damage risks as usual and the increased risks due to climate change as well. On the basis of Eqn.(5-3), the cost contributes to three part, 1) mitigating corrosion risk due to climate change, 2) increasing corrosion resistance, and 3) offsetting the loss of adaptation effectiveness due to climate change. Table 5-1 gives the subdivision of the cost related to the three parts.

Table 5-1 Subdivision of the cost of the adaptation/maintenance measures for chloride-induced corrosion of Bridge BB1 (1925) in Sydney

Adaptation/Maintenance Measures	Percentage of total cost to mitigate increased risk due to climate change	Percentage of the total cost to increase corrosion resistance	Percentage of the total cost to offset the loss of adaptation effectiveness due to climate change
Polyurethane sealer	47%	7%	46%
p-m cementious coating	31%	46%	23%
Chloride extraction	29%	53%	18%

Replacement	22%	78%	0%
Cathodic protection	22%	78%	0%

For an example, for p-m cementious coating, 31% of the total cost is contributed to the mitigation of increased corrosion risk due to climate change, 46% is contributed to improve the resistance of concrete structures to chloride attack, and 23% is contributed to the loss of the effectiveness of adaptation options due to climate change. For polyurethane, nearly a half of cost is actually for offsetting the loss of its effectiveness due to climate change.

It should be pointed out that the cathodic protection in the table is assumedly not affected by the climate change. In fact, its effectiveness may be affected by sea level rise, which will not be discussed in this report.

Finally, Figure 5-4 indicates the overall effectiveness of adaptation options under changing climate in relation to the cost considering a discount rate of 3%. The width of the bar represents the relative adaptation effectiveness of each option. Polyurethane sealer is least effective.

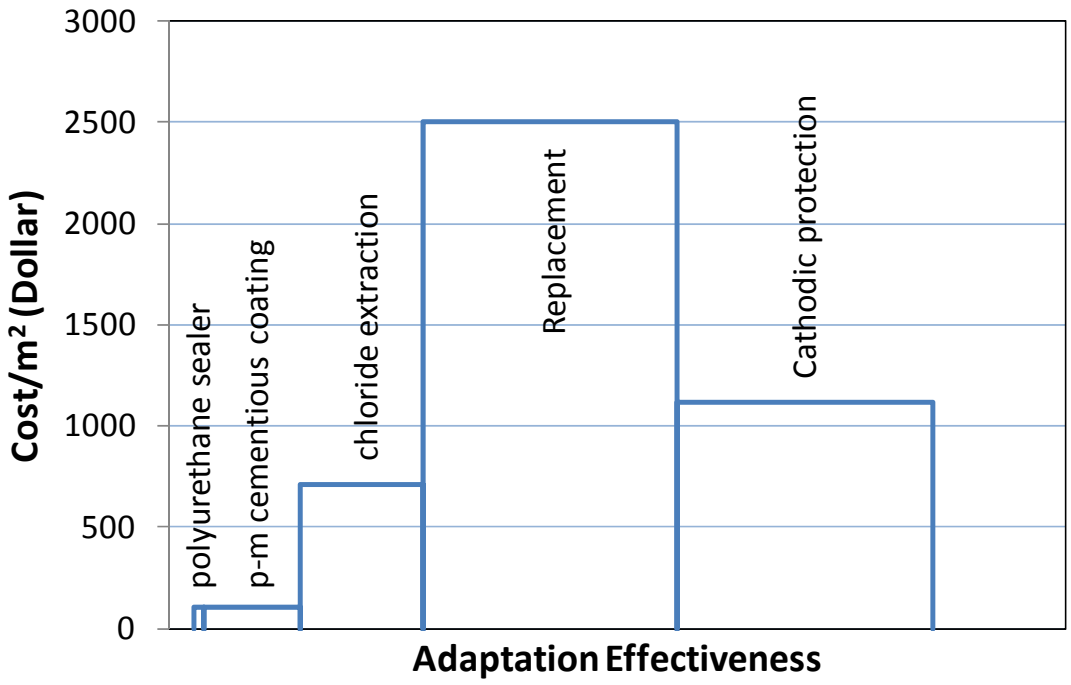

Figure 5-4 Cost and effectiveness of adaptation options for chloride-induced corrosion of concrete structures of Bridge BB1 (1925) in NSW, at a discount rate of 3%.

5.3.2 Bridges BD2 Constructed in 1967 in Northern Region

Figure 5-5 describes the effect of adaptation measures (1)-(4) described above on the probability of corrosion initiation and damage as well as rebar loss. It appears the most effective approach is the use of p-m cementious coatings on the surface of 62mm cover

of concrete that already meets the current design stands for structures at exposure C2. The measure not only counteracts the impact of climate change, but also enough to maintain the probability of corrosion initiation and damage at a reasonably low level.

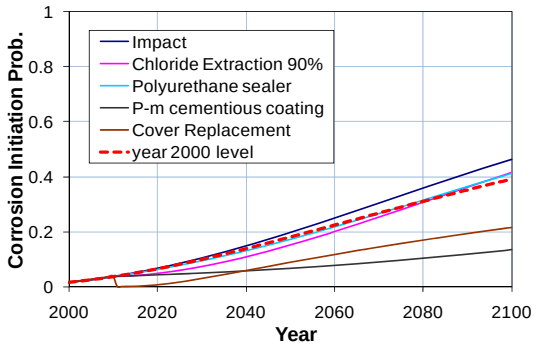

(a) Corrosion initiation probability

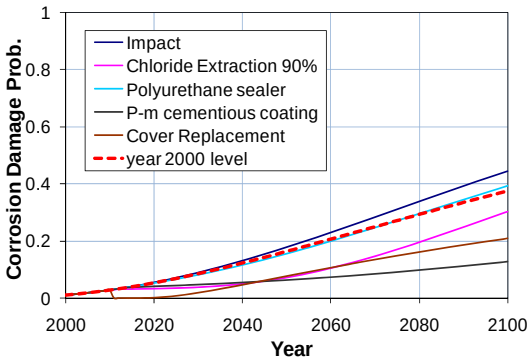

(b) Corrosion damage probability

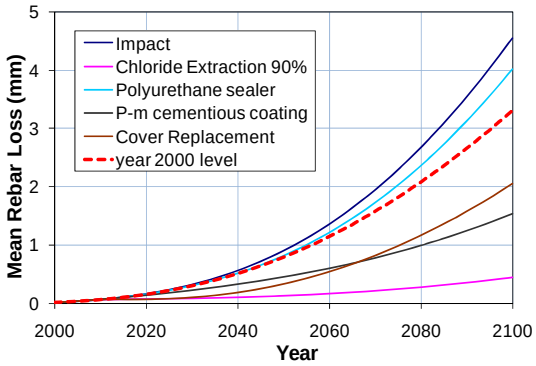

(c) Mean rebar loss (mm)

Figure 5-5 Probability of chloride-induced corrosion initiation and damage and mean rebar loss of concrete structures of Bridge BD2 (1967) in northern region NSW considering adaptation options (1)-(4). 'Impact' - with the effect of climate change; 'Year 2000 level' – the relevant value in the absence of climate change. (The probability is represented by decimal numbers)

The second most effective approach is cover replacement that assumes the same cover thickness but at lower rate of penetration. Although it is still projected that there is an increase in the probability of corrosion initiation and damage, but it maintains the probability of corrosion initiation below the estimation in the absence of climate change until 2080, and maintains the probability of corrosion damage below the projection in the absence of climate change. In others word, it has at least mitigated the impact of climate change.

Considering a service life of concrete structure till 2100, the cost and cost/benefit ratio is shown in Figure 5-6. Once again, the ratio is just a relative indicator for the purpose of comparison. As shown in the figure, cover replacement is most expensive and also highest cost/benefit among the five options, while p-m cementious coating is the least. Different from the last case, the use of polyurethane coating appears also much lower in addition to its lower sensitivity to the discount rate.

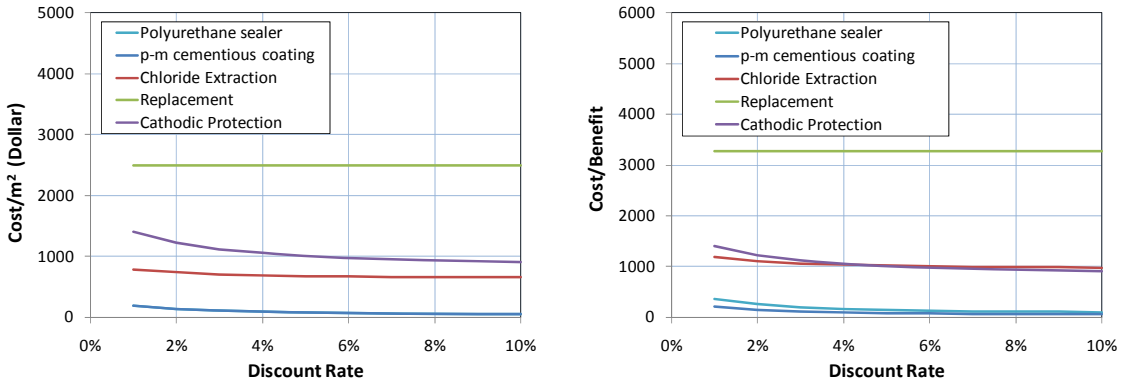

(a) Cost (b) Cost/Benefit

Figure 5-6 Cost (AU$) and cost/benefit in relation to discount rate for the implementation of adaptation options for chloride-induced corrosion of concrete structures of Bridge BD2 (1967) in northern regions of NSW under climate change.

Table 5-2 gives the subdivision of the cost related to the three parts. Comparing to the previous case, polyurethane sealer is much more effective with 29% of the total cost is contributed to the mitigation of increased corrosion risk due to climate change, 57% is contributed to improve the resistance of concrete structures to chloride attack, and moderate 14% is contributed to the loss of the effectiveness of adaptation options due to climate change. In general, more than a half of the total cost goes to increase the resistance to corrosion.

Table 5-2 Subdivision of the cost of the adaptation/maintenance measures for chloride-induced corrosion of Bridges BD2 (1967) in the northern region of NSW.

Adaptation/Maintenance Measures	Percentage of total cost to mitigate increased risk due to climate change	Percentage of the total cost to increase corrosion resistance	Percentage of the total cost to offset the loss of adaptation effectiveness due to climate change
Polyurethane sealer	29%	57%	14%
p-m cementious coating	22%	74%	4%
Chloride extraction	26%	64%	10%
Replacement	25%	69%	6%
Cathodic protection	22%	78%	0%

Once again, it should be pointed out that the cathodic protection in the table is assumedly not affected by the climate change. However, its effectiveness may be affected by sea level rise, which will not be discussed in this report.

In addition, Figure 5-7 indicates the overall effectiveness of adaptation options under changing climate in relation to the cost with considering a discount rate of 3%. In the

figure, the width of each bar represents the relative adaptation effectiveness of each option, while the height represents the cost. For this case, p-m cementious coating becomes a very attractive option with low cost and high effectiveness. On the other hand, cover replacement is least attractive with high cost and relatively low effectiveness.

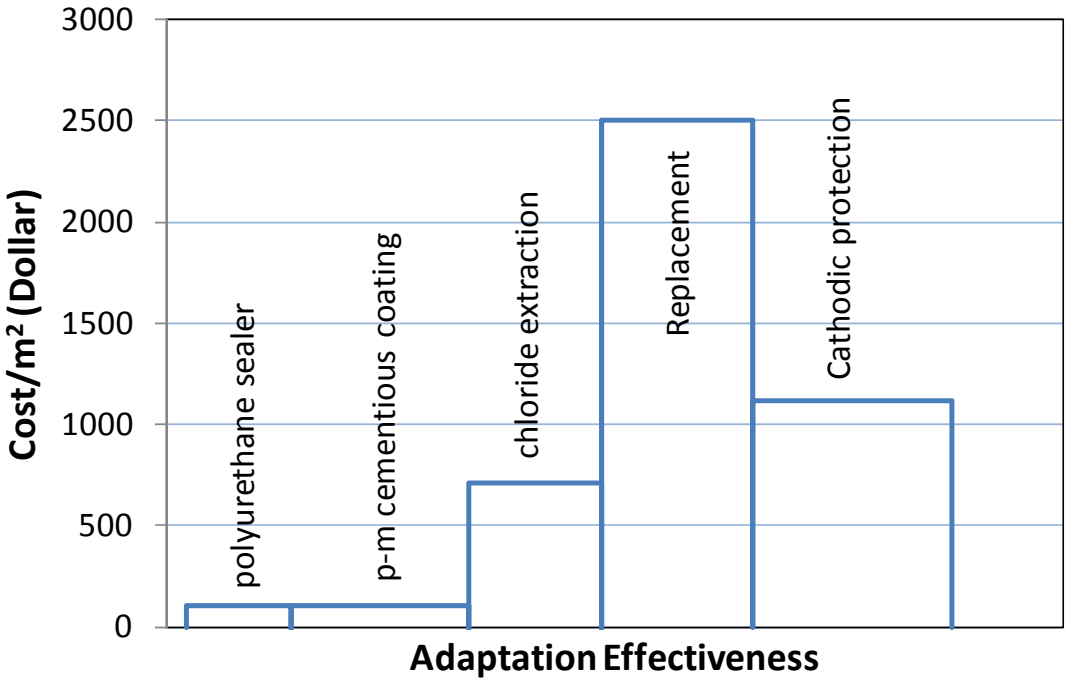

Figure 5-7 Cost and effectiveness of adaptation options for chloride-induced corrosion of concrete structures of Bridge BD2(1967) in the northern region of NSW, at a discount rate of 3%.

5.3.3 Concrete Slab Soffits in Port Townsville

Figure 5-8 describes the effect of adaptation measures (1)-(4) described above on the probability of corrosion initiation and damage as well as rebar loss of concrete slabs in one of berths in Port of Townsville. It appears the most effective approach to reduce the corrosion is the use of either cover replacement or p-m cementious coatings, though the probability corrosion initiation and damage increase again to almost 30% by 2100 under A1FI emission scenario.

Other approaches including chloride extraction that only marginally reduces the probability of corrosion initiation and damage. The use of polyurethane sealer cannot even maintain the probability below the estimation in the absence of climate change.

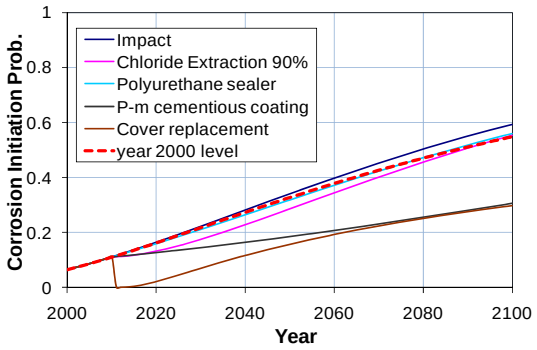

(d) Corrosion initiation probability

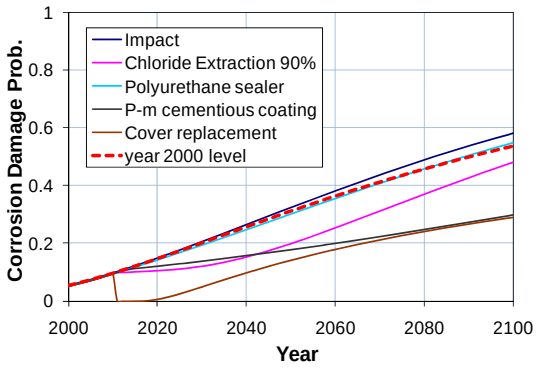

(e) Corrosion damage probability

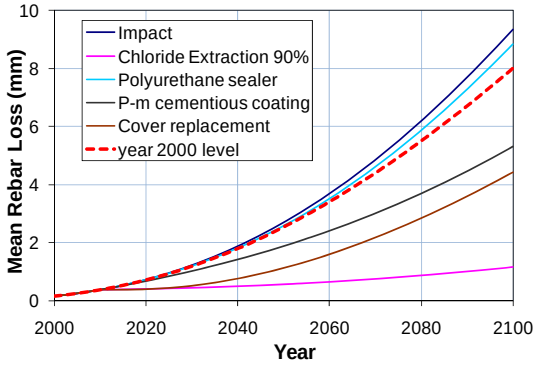

(f) Mean rebar loss (mm)

Figure 5-8 Probability of chloride-induced corrosion initiation and damage and mean rebar loss of structures of concrete slab in Port of Townsville considering adaptation options (1)-(4). 'Impact' - with the effect of climate change; 'Year 2000 level' – the relevant value in the absence of climate change. (The probability is represented by decimal numbers)

Considering a service life of concrete slab structure till 2100, the cost and cost/benefit ratio is shown in Figure 5-9. As seen, cover replacement is most expansive and also highest cost/benefit among the five options, while p-m cementious coating is the least. It also indicates that the cost/benefit ratio to use polyurethane coating appears sensitive to the discount rate.

Table 5-3 gives the subdivision of the cost related to the three parts. As seen, polyurethane sealer is less effective with 36% of the total cost contributed to the loss of the effectiveness of adaptation options due to climate change. Meanwhile, 38% of the total cost is contributed to the mitigation of increased corrosion risk due to climate change, and 25% is contributed to improve the resistance of concrete structures to chloride attack. In general, except of polyurethane sealer, more than a half of the total cost of all options goes to increase the resistance to corrosion, especially cathodic protection and p-m cementious coating that is as high as 87% and 75%, respectively. In other words, the adaptive capacity will be significantly strengthened to resist chloride-induced corrosion.

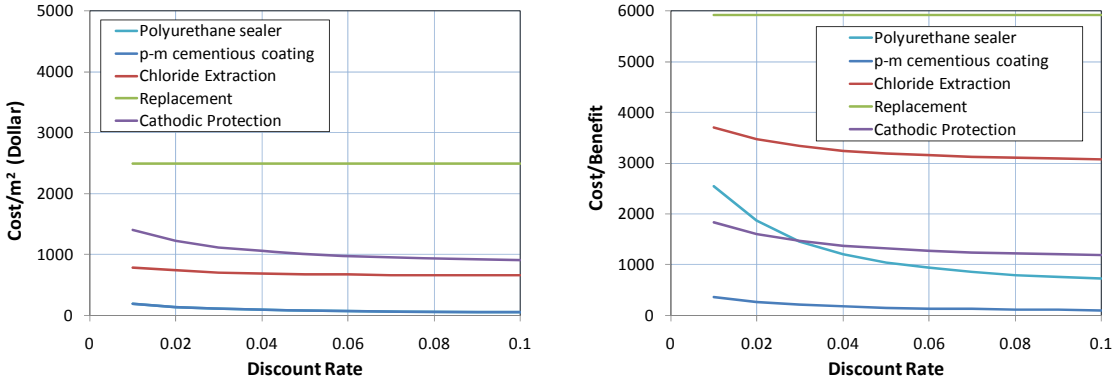

(a) Cost (b) Cost/Benefit

Figure 5-9 Cost (AU$) and cost/benefit in relation to discount rate for the implementation of adaptation options for chloride-induced corrosion of a concrete slab in Port of Townsville under climate change.

Table 5-3 Subdivision of the cost of the adaptation/maintenance measures for chloride-induced corrosion of concrete slab of port structure in the port of Townsville.

Adaptation/Maintenance Measures	Percentage of total cost to mitigate increased risk due to climate change	Percentage of the total cost to increase corrosion resistance	Percentage of the total cost to offset the loss of adaptation effectiveness due to climate change
Polyurethane sealer	38%	25%	36%
p-m cementious coating	16%	75%	9%
Chloride extraction	28%	51%	21%
Replacement	20%	71%	8%
Cathodic protection	13%	87%	0%

As discussed before, the cathodic protection in the table is assumedly not affected by the climate change, which may indeed be affected by sea level rise. However, it will not be discussed in this report.

Figure 5-10 describes the overall effectiveness of adaptation options under changing climate in relation to the cost with considering a discount rate of 3%. In the figure, the width of each bar represents the relative effectiveness of each adaptation option, while the height represents the cost. For this case, cathodic protection and p-m cementious coating becomes two options to effectively mitigate chloride-induced corrosion under changing climate.

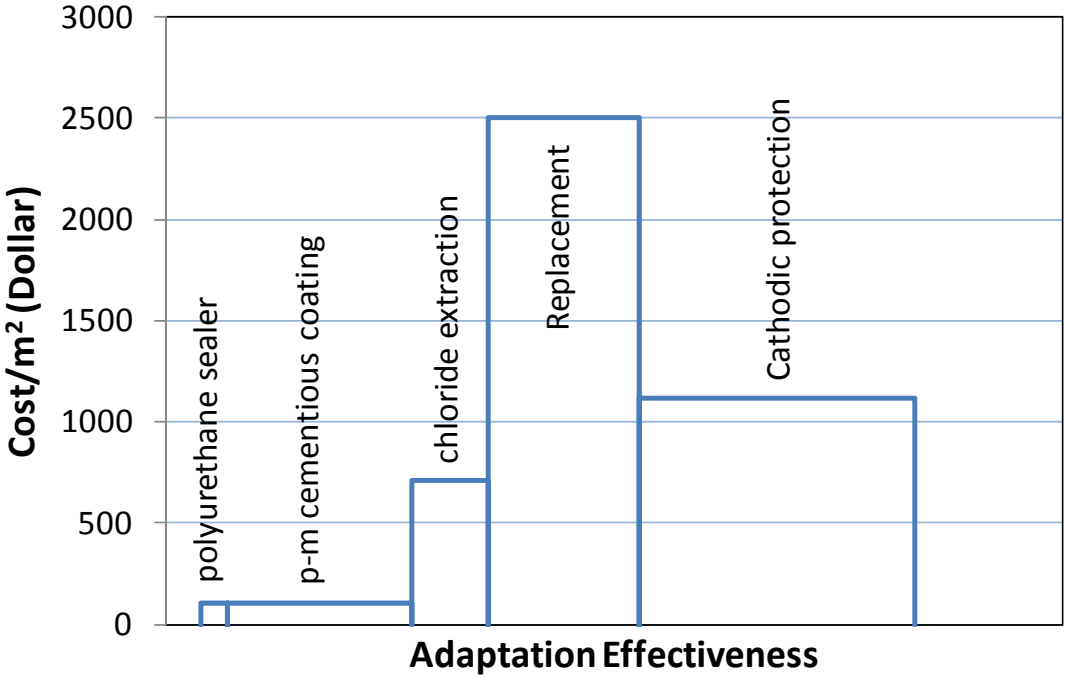

Figure 5-10 Cost and effectiveness of adaptation options for chloride-induced corrosion of concrete slab structures in the Port of Townsville at a discount rate of 0.03.

5.4 Adaptation Assessment for Carbonation-Induced Corrosion and Cost/Benefit

5.4.1 Concrete Slab Soffits in Port Townsville

Figure 5-11 describes the effect of adaptation measures (6)-(8) introduced above on the the probability of corrosion damage of concrete slabs in one of berths in Port of Townsville. Considering that the acrylic-based surface coating is normally applied in dry environment, only two options, realkanisation and cover replacement, are considered for the concrete slab at exposure C2. Realkalisation is an electrochemical process to raise pH near reinforcement. After realkanisation, concrete will not easily recarbonate. It is therefore assumed that corrosion will stop permanently. Meanwhile, cover replacement also stops corrosion while it may not stop carbonation.

Considering a service life of concrete slab structure till 2100, the cost and cost/benefit ratio is shown in Figure 5-9. As seen, cover replacement is most expansive and also highest cost/benefit among the five options, while p-m cementious coating is the least. It also indicates that the cost/benefit ratio to use polyurethane coating appears sensitive to the discount rate.

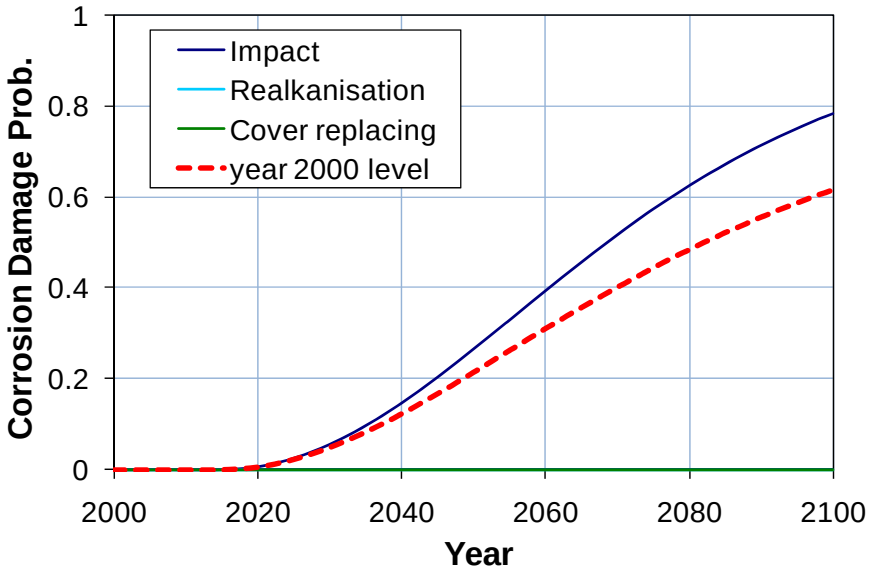

Figure 5-11 Probability of carbonation-induced corrosion damage of structures of concrete slab in Port of Townsville considering adaptation options (6) and (8). 'Impact' - with the effect of climate change; 'Year 2000 level' – the relevant value in the absence of climate change. (The probability is represented by decimal numbers; curves for realkanisation and cover replacing are almost zero for the period)

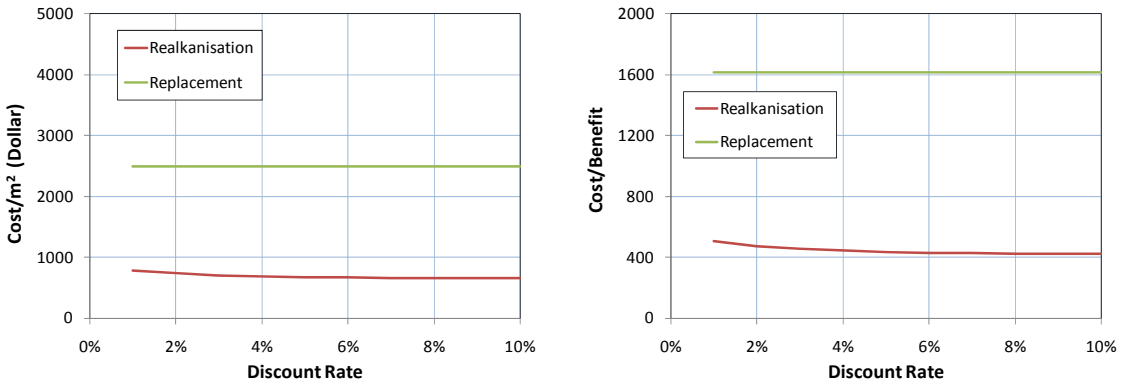

Figure 5-12 Cost (AU$) and cost/benefit in relation to discount rate for the implementation of adaptation options for carbonation-induced corrosion of a concrete slab in Port of Townsville under climate change.

Table 5-4 gives the subdivision of the cost related to the three parts. As seen, both alkanisation and cover replacement 38% of the total cost contributed to the mitigation of increased corrosion risk due to climate change, and other 62% is contributed to improve the resistance of concrete structures to chloride attack or adaptive capacity. However, their cost to reach that effectiveness is different.

Figure 5-13 describes the overall effectiveness of adaptation options under changing climate in relation to the cost with considering a discount rate of 0.03. In the figure, the width of each bar represents the relative effectiveness of each adaptation option for carbonation-induced corrosion, while the height represents the cost. For this case,

realkanisation has the advantage over the cover replacement to effectively mitigate chloride-induced corrosion under changing climate. due to its low cost.

Table 5-4 Subdivision of the cost of the adaptation/maintenance measures for carbonation-induced corrosion of concrete slab of port structure in the port of Townsville.

Adaptation/Maintenance Measures	Percentage of total cost to mitigate increased risk due to climate change	Percentage of the total cost to increase corrosion resistance	Percentage of the total cost to offset the loss of adaptation effectiveness due to climate change
Realkanisation	38%	62%	0%
Cover replacement	38%	62%	0%

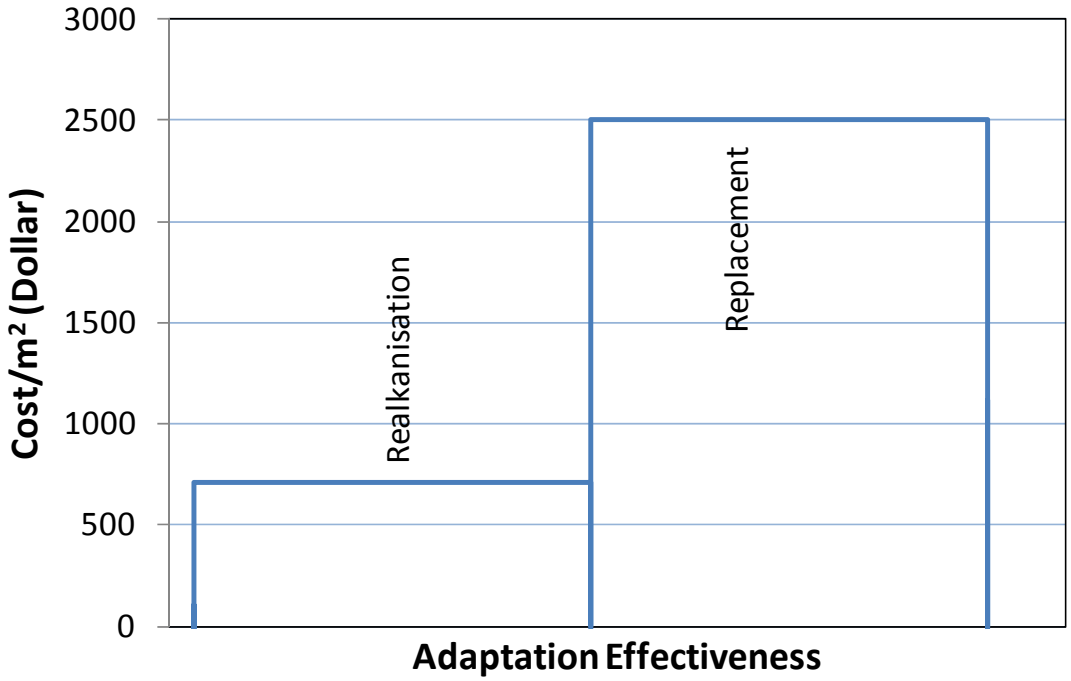

Figure 5-13 Cost and effectiveness of adaptation options for carbonation-induced corrosion of concrete slab structures in the Port of Townsville at a discount rate of 3%.

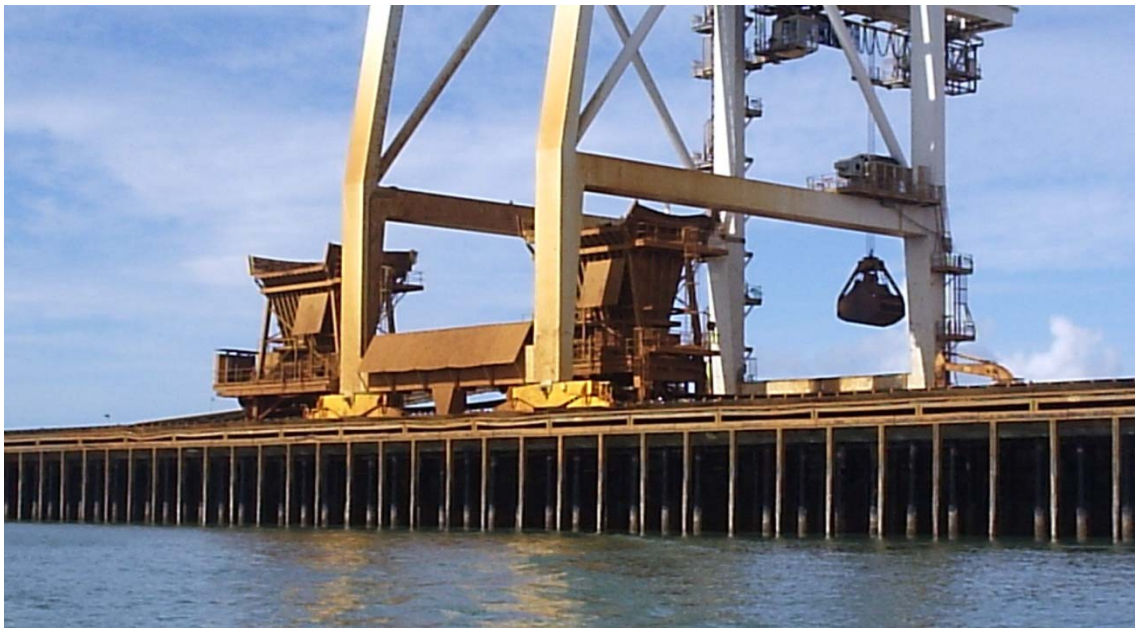

Port (source: CSIRO)

6. SUMMARY

Since most designs of existing concrete structures do not take into account the effect of a changing environment, there are concerns that many existing concrete infrastructure are likely to suffer from decreased durability, safety and serviceability.

This report has established a probabilistic simulation approach based on chloride- and carbonation-induced corrosion models that can be calibrated by the historical field measurement of chloride concentration and carbonation penetration and then can project the probability of corrosion initiation and damage into future. We developed models of adaptation options and looked at their effects on various parameters of corrosion models for existing concrete structures, such as carbonation depth and carbon dioxide diffusion coefficient for carbonation-induced corrosion, and chloride concentration, chloride diffusion coefficient, critical chloride concentration for chloride-induced corrosion, and corrosion rate. These models were then applied to simulate the corrosion under the influence of adaptation measure, including surface coating, alkanisation, chloride extraction, cover replacement, cathodic protection and so on. The effect of climate change is also considered in the models through the influence of carbon dioxide concentration, temperature and relative humidity.

Two typical concrete structures, bridges and port structures, are used as case studies to elucidate the impact of climate change on existing concrete structures and available options as well as their effectiveness in reducing the impact of climate change and increasing adaptive capacity to counteract corrosion. The investigated bridges are located in Sydney, Southern, Northern and Hunter regions of NSW and constructed during the period of pre-1959, 1959-1970, 1971-1994 and post-1995. At the same time, the investigated port structures are concrete slab soffits and columns from a berth that is

managed by Port of Townsville Limited. As found, although all investigated structures are under exposure C2, the concrete cover does not necessarily meet the current standard, such as AS 3600-2009, that requires 65mm. In fact, the cover of the most of existing bridges in this case study is less than 65mm, with one reaching as low as 29mm. This explained more on the importance to specifically assess durability of existing bridges and especially when considering the impact of climate change on the durability in relation to carbonation- and chloride-induced corrosion.

In the part 2 of the report, it is indicated that the effect of climate change on chloride-induced corrosion of concrete structures which design follows the AS3600 and AS5100.5, is within an increase of 3.5 percentage points in probability by 2100. In practice, the change of the probability can go higher due to non-binding on the standards or lack of quality assurance in construction, for example, use of lower concrete cover. The bridges in Sydney, constructed in 1925 with 29mm cover, shows that the climate change at A1FI emission scenario can leads up to an 8 percentage points increase in corrosion initiation and damage probability, or equivalent 13% increase in percentage change. Even for a modern bridge in the northern region of NSW, constructed in 1984, the structure on the bridge at exposure C1 and C2 may experience up to 5-7 percentage points increase in probability by 2100 in the presence of climate change impact at A1FI emission scenario.

Due to an improper concrete cover of some of the early constructed bridges, climate change may lead to a considerable impact on carbonation-induced corrosion. For example, a bridge constructed in 1925 in Sydney has only 29mm concrete cover. The probability of corrosion initiation is 72, 67 and 63 percentage points by 2100 for A1FI, A1B and 550 ppm stabilisation emission scenarios, respectively, in comparison with 51 percentage points estimated in the absence of climate change. In another word, the probability increases 21, 16 and 12 in probability, or an equivalent percentage increase of 41%, 31% and 14% due to climate change. Meanwhile, the probability of corrosion damage is 63, 60 and 55 percentage points in comparison with 44 percentage points estimated in the absence of climate change, also a significant increase due to climate change. For a concrete column at exposure C2 in Port Townsville, climate change impact may lead to an increase in probability of carbonation induced corrosion initiation form 1 to 45 percentage points for A1FI emission scenario, 28 percentage points for A1B emission scenario and 14 percentage points for 550 ppm stabilisation emission scenario by 2100. It also leads to the increase corrosion damage probability from 0.2 to 16, 8.8 and 4.0 percentage points respectively for the three emission scenarios by 2100.

Both chloride-induced and carbonation-induced corrosion show the potential for a scalable impact of climate change, which should be considered for maintenance planning. Adaptation options should also be developed and optimised to mitigate the impact and enhance the adaptive capacity of concrete structures to changing climate.

In the simulation of implementation of adaptations to counteract the impact of climate change, five options including electrochemical chloride extraction, polyurethane sealer, polymer-modified cementious coating, cover replacement and cathodic protection, were considered to reduce chloride-induced corrosion. Other two options including realkalisation and cover replacement were introduced to mitigate carbonation-induced

corrosion. Meanwhile, cost and adaptation effectiveness are also introduced to quantify the adaptation options for the identification of the most preferable option in association with a specific concrete structure, such as a slab or column. The cost includes initial implementation cost and on-running operating cost, which are all converted to their present value in 2011 with a discount rate ranging from 1% to 10% selected for sensitivity assessment. The effectiveness, also known as a proxy of benefit due to the implementation of adaptation options, is defined as the amount of reduction in corrosion risk from 'business as usual (BAU)' after implementing adaptations. As a result, adaptation effectiveness diagram is developed by combining cost with adaptation effectiveness, which may facilitate the decision-making in developing adaptation strategies that maximise adaptation effectiveness with minimised cost.

The cost contributes to three factors, i.e. 1) reducing the impact of climate change, 2) increasing adaptive capacity to resist corrosion, and 3) offsetting the loss of adaptation effectiveness due to climate change. In general, the more there is more on offsetting, less effective is the option. The case study of concrete bridges indicates that the replacement of concrete cover is often to be the most effective options, but it is also the most expensive one. Surface coating is the least costly, but is usually, but not always relatively less effective. For the bridge constructed in 1925 in Sydney, cathodic protection is the preferred adaptation measure to mitigate the chloride-induced corrosion damage due to its greater effectiveness and moderate cost. Among the total cost, 22% is contributed to mitigate the increase corrosion damage risk due to climate change, 78% is contributed to increase adaptive capacity to resist corrosion, and nothing is contributed to offset the loss of adaptation effectiveness due to climate change. It should be pointed out the effectiveness of cathodic protection may be affected by sea level rise that may change the cost for offset the loss of effectiveness. At the same time, the use of polyurethane sealer is the least preferred due to its very low effectiveness though low cost. For this, 46% of the total cost is contributed to offset the loss, which is not really beneficial to the enhancement of adaptive capacity to counteract corrosion damage.

Depending on the residual risk of corrosion damage of concrete structure after implementing adaptation options, the preferred adaptation option can vary. For a bridge constructed in 1967 in the northern region of NSW, polymer-modified cementious coating appears the most preferable due to its great effectiveness with 24% of the total cost is contributed to mitigate the increasing risk as a result of climate change, 57% is contributed to strengthen the adaptive capacity, and only 4% is contributed to offset the loss of adaptation effectiveness, in comparison with 14% for polyurethane sealer, 10% for cathodic protection. Meanwhile, it has a cost much lower than cover replacement, cathodic protection and chloride extraction.

A similar approach was applied for the cost/benefit assessment of adaptation options for carbonation-induced corrosion of port structures in relation to realkalisation and cover replacement are considered.

As reported in part 2 of the report, the climate change impact assessment on the aspect of design that follows the Australian standards may provide general rules for concrete structural design taking into account effects of changing climate. Different from that,

impacts on existing concrete infrastructure and the adaptation that should be applied to mitigate the impact are specific due to the uniqueness of individual structures especially regarding their different local environment exposure history as well as the uncertainties in construction and maintenance. Therefore, an effective adaptation option should be developed at the level of individual concrete structures. Finally, cost and benefit assessment should further be developed to also consider damage and repair costs, and the cost-effectiveness of 'business as usual' (do nothing) by utilising life-cycle cost assessment of concrete infrastructure.

ACKNOWLEDGMENTS

The authors thank the Department of Climate Change and Energy Efficiency (DCCEE) and the CSIRO Climate Adaptation Flagship for funding this research.

The authors also express their appreciation to Jo Mummery, Catherine Farrell, Robert Davitt, Mark Eslake and Ian Foster of DCCEE, Allen Kearns, Seona Meharg, Yong-Bing Khoo, Phillip Paevere, and Greg Foliente of CSIRO, Palitha Manamperi, Michael Moore, Siva Perumynar, Farhana Jesmin and Jocob Craig of the Road Transport Authority, Kim Cope and Robert Renn of the Port of Melbourne Corporation, Kate Johnson and Robert Henaway of Port of Townsville Limited, and Roger Jones of the University of Victoria for their valuable advice and generous support. The authors also appreciate the assistance of Dr Xiaoli Deng and Michael Netherton from the University of Newcastle. Finally, the authors thank all members of the project's expert panel for their inputs.

REFERENCES

Aguair, J.B., Camoes, A. and Moreira, P.M. (2008), Coatings for Concrete Protection Against Aggressive Environments, *Journal of Advanced Concrete Technology*, 6(1): 243-250.

Al-Khaiat, H. and Fattuhi, N. (2002), Carbonation of Concrete Exposed to Hot and Arid Climate, *Journal of Materials in Civil Engineering*, 14(2): 97-107.

Al-Khayat, H., Haque, M.N. and Fattuhi, N.I. (2002), Concrete Carbonation in Arid Climate, *Materials and Structures*, 35: 421-426.

Andrade, C., Diez, J.M. and Alonso, C. (1997), Mathematical Modeling of a Concrete Surface "Skin Effect" on Diffusion in Chloride Contaminated Media, *Advances in Cement Based Materials*, 6: 39-44.

Ang, A. H-S. and Tang, W.H. (2007), P*robability Concepts in Engineering: Emphasis on Applications to Civil and Environmental Engineering*, Wiley.

Bamforth, P. B., Price, W. F. and Emerson, M. (1997) *International Review of Chloride Ingress into Structural Concrete: A Tri-report (TRL report)*, Transport Research Laboratory, Scotland.

Barnes, R. and Zheng, T. (2008), Research on Factors Affecting Concrete Cover Measurement, *NDT.net - The e-Journal of Nondestructive Testing*, December 2008.

Bentur, A., Diamond, S. and Berke, N.S. (1997), *Steel Corrosion in Concrete*, E&FN Spon, London.

BRE (2003), *Residual Life Models for Concrete Repair - Assessment of the Concrete Repair Process*, Building Research Establishment, UK.

Broomfield, J.P. (1997), *Corrosion of Steel in Concrete*, E&FN Spon, London.

BS 1881-Part 124 (1988), *Testing concrete - Part 124: Methods for Analysis of Hardened Concrete*, British Standards, U.K.

BS1881-Part 204 (1988), *Testing Concrete: Recommendations on the Use of Electromagnetic Covermeters*, British Standards, U.K.

Buenfeld, N.R. and Zhang, J.-Z. (1998), Chloride Diffusion Through Surface-Treated Mortar Specimens, *Cement and Concrete Research*, 28(5): 665-674.

DuraCrete (2000a), Statistical Quantification of the Variables in the Limit State Functions, DuraCrete - Probabilistic Performance based Durability Design of Concrete

Structures, EU - Brite EuRam III, Contract BRPR-CT95-0132, Project BE95-1347/R9, January 2000, 130 p.

DuraCrete (2000b), Probabilistic Calculations, DuraCrete - Probabilistic Performance based Durability Design of Concrete Structures, EU - Brite EuRam III, Contract BRPR-CT95-0132, Project BE95-1347/R12-13, May 2000, 41 p.

fib (2006), *Model Code for Service Life Design*, fib, Bulletin 34, February 2006, Lausanne.

Ho, D.W.S. and Harrison, R.S. (1990), Influence of Surface Coatings on Carbonation of Concrete, *Journal of Materials in Civil Engineering*, ASCE, 2(1): 35-44.

Ibrahim, M., Al-Gahtani, A.S., Maslehuddin, M. and Dakhil, F.H. (1999), Use of Surface Treatment Materials to Improve Concrete Durability, *Journal of Materials in Civil Engineering*, ASCE, 11(1): 36-40.

Ihekwaba, N.M., Hope, B.B. and Hansson, C.M. (1996), Carbonation and Electrochemical Chloride Extraction from Concrete, *Cement and Concrete Research*, 26(7): 1095-1107.

IPCC (2007), *Fourth Assessment Report of the Intergovernmental Panel in Climate Change*, Cambridge University Press, UK.

Jones, M.R., Dhir, R.K., Newlands, M.D. and Abbas, A.M.O. (2000), A Study of the CEN Test Method for Measurement of the Carbonation Depth of Hardened Concrete, *Materials and Structures*, 33: 135-142.

Kershel, O.M. (2009), *Influence of Spatial Variability on Whole Life Management of Reinforced Concrete Bridges*, PhD Thesis, University of Dublin, Trinity College.

McGee, R. (1999), Modelling of Durability Performance of Tasmanian Bridges, *ICASP8 Applications of Statistics and Probability in Civil Engineering*, R.E. Melchers and M.G. Stewart (eds.), 1: 297-306.

Moreno, E.I., Solis-Carcano, R.G., Serrano-Ixtepan, D. and Arias-Palma, C.A. (2007), Performance of Concrete Coatings Against Carbonation-Induced Corrosion, *Corrosion 2007*, NACE, Paper No. 07297.

Polder, R.B. and de Rooij, M.R. (2005), Durability of Marine Structures - Field Investigations and Modelling, *HERON*, 50(3): 133-153.

Port of Townsville (2009). Design of a New Ship Loader and Augmentation Work. Report prepared by Hyder Consulting Pty Ltd.

RTA (2008), Report: Global Durability Study of RTA Concrete Coastal Bridges - Stage 1. Report A., Bridge Technology, Roads and Traffic Authority of NSW, Australia.

Russell, D., Basheer, P.A.M., Rankin, G.I.B. and Long, E.A. (2001), Effect of Relative Humidity and Air Permeability on Prediction of the Rate of carbonation of Concrete, *Proceedings of the Institution of Civil Engineers*, 146(3): 319-326.

Schneck, U., Winkler, T. and Grunzig, H. (2007), Chloride Extraction from Reinforced Concrete - a New Defined Way of Application, *Corrosion of Reinforcement in Concrete*, M. Raupach, B. Elsener, R. Polder and J. Mietz (eds), CRC Press, 263-276.

Sharp, S.R., Clemena, G.G., Virmani, Y.P., Stoner, G.E. and Kelly, R.G. (2002), Electrochemical Chloride Extraction: Influence of Concrete Surface on Treatment, Report No. FHWA-RD-02-107, Federal Highway Administration, September 2002.

Song, H-W., Lee, C-H. and Ann, K.Y. (2008), Factors Influencing Chloride Transport in Concrete Structures Exposed to Marine Environments, *Cement & Concrete Composites*, 30: 113-121.

Stewart, M.G. (2010), Computer Program CIRCAA-RC-EXISTING(Climate Impact Risks for Corrosion Adaptation Assessment - RC - Existing Structures), Climate Change Impact and Adaptation on Concrete Infrastructure Deterioration - Phase II, Manual, V2.0, Centre for Infrastructure Performance and Reliability, The University of Newcastle, September 2010.

Swamy, R.N., Suryavanshi, A.K. and Tanikawa, S. (1998), Protective Ability of an Acrylic-Based Surface Coating System Against Chloride and Carbonation Penetration into Concrete, *ACI Materials Journal*, 95(2): 101-112.

Tamimi, A.K., Abdalla, J.A. and Sakka, Z.I. (2008), Prediction of Long Term Chloride Diffusion of Concrete in Harsh Environment, *Construction and Building Materials*, 22: 829-836.

Val, D.V. and Stewart, M.G. (2003), Life Cycle Cost Analysis of Reinforced Concrete Structures in Marine Environments, *Structural Safety*, 25(4): 343-362.

Velivasakis, E.E., Henriksen, S.K. and Whitmore, D. (1998), Chloride Extraction and Realkanization of Reinforced Concrete Stop Steel Corrosion, *Journal of Performance of Constructed Facilities*, ASCE, 12(2): 77-84.

Yeih, W. and Chang, J.J. (2005), A Study on the Efficiency of Electrochemical Realkanization of Carbonated Concrete, *Construction and Building Materials*, 19(7): 516-524.

Yoon, I.S., Copuroglu, O., and Park, K.B. (2007). Effect of global climatic change on carbonation progress of concrete. *Atmospheric Environment*, 41: 7274-7285.

Contact Us
Phone: 1300 363 400
+61 3 9545 2176
Email: enquiries@csiro.au
Web: www.csiro.au

Your CSIRO

Australia is founding its future on science and innovation. Its national science agency, CSIRO, is a powerhouse of ideas, technologies and skills for building prosperity, growth, health and sustainability. It serves governments, industries, business and communities across the nation.